R.A.F.T.

Vertical Takeoff Rescue Amphibious Firefighting Tiltrotor

Virginia Tech

Virginia Polytechnic Institute
and State University

May 2010

NASA Tiltrotor Design Report

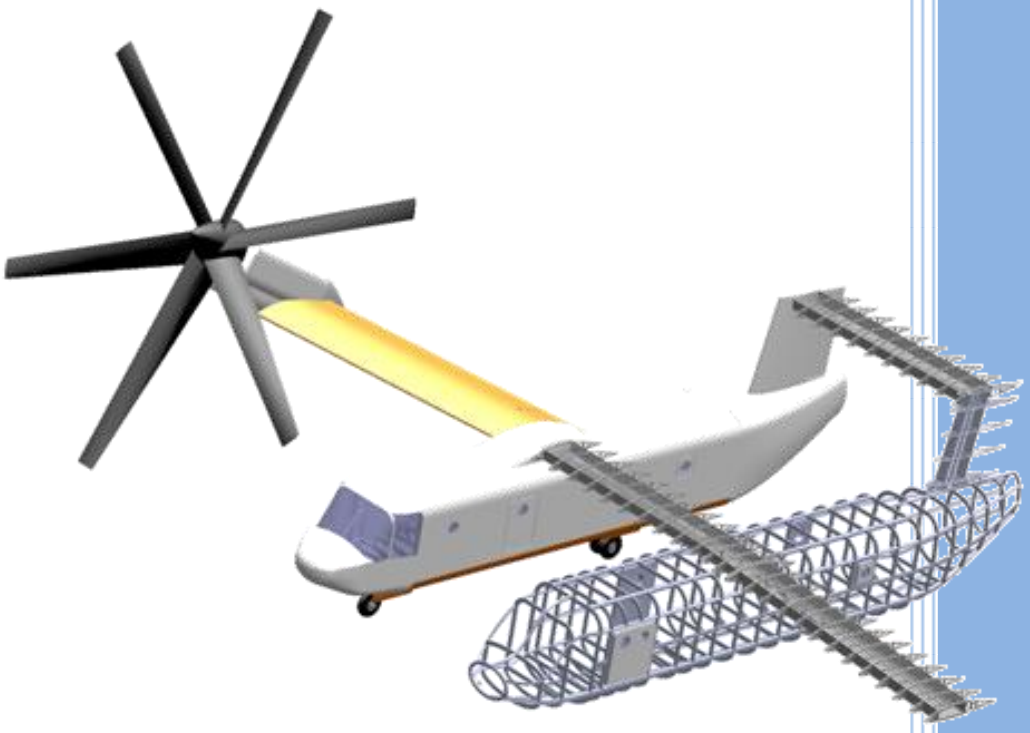

Faculty Advisor : Dr. William Mason
Team Lead: Michael Creaven

II. Team Members

From left to right:

James Tenney – Undergraduate, Senior

Jason Smith – Undergraduate, Senior

Alan Steinert – Undergraduate, Senior

Ryan Paetzell – Undergraduate, Senior

Meagan Hom – Undergraduate, Senior

Joseph Diner – Undergraduate, Senior

Ryan Berg – Undergraduate, Senior

Michael Creaven – Undergraduate, Senior

Alexander Carra - Undergraduate, Senior

Bryant Tomlin – Undergraduate, Senior

III. Abstract

The design of the proposed amphibious tiltrotor aircraft was conducted by a team of 10 undergraduate students as a capstone design project. The aircraft was designed to meet requirements specified by the NASA Amphibious Tiltrotor Competition. The aircraft is required to take off and land vertically on both water and land, as well as having an 800 nm range and a cruise speed of 300 kts. The payload is up to 50 passengers or water for firefighting operations. Specifics such as the operational sea state, maximum altitude, and total water capacity were later defined by the study based on currently existing aircraft and technical analysis.

A dual fuselage concept, named the Vertical Transport Rescue Amphibious Firefighting Tiltrotor (V.T. R.A.F.T.) was proposed as the design best suited to fulfill the mission. The aircraft can perform vertical flight operations with a maximum takeoff gross weight (TOGW) of 62,460 lb. The aircraft can accommodate 50 passengers or 12,000 lb of water, in addition to 10,175 lb of fuel. Two 6150 shp turboshaft engines power the aircraft. Each engine is located at the wingtip inside the nacelles, which are capable of rotating at a rate of 3.0°/sec. This allows the aircraft to change from helicopter mode to airplane mode in 30 sec. The main cabin is not pressurized; however, for high altitude operations without passengers oxygen is supplied to the flight crew.

Water stability in a sea state of up to four was a major concern and was instrumental in the choice of a dual fuselage concept. This configuration eliminates the need for pontoons, which reduces drag and aircraft complexity. Additionally, the dual fuselage design reduced aerodynamic loading on the main spar and enhanced aerial rescue capabilities by providing a rescue area shielded from the rotor downwash.

Although not mandated by the competition, the aircraft is designed to be able to receive aerial refueling and perform aero-medical operations. In addition to vertical takeoff and landing the aircraft is designed to perform a short takeoff from land based facilities, increasing the TOGW to 70,000 lb. Future study and analysis should be conducted to determine the engines capacity to avoid the ingestion of water mist while hovering over water as well as further investigation of wing flutter phenomenon for this design.

IV. Letter from the Advisor

The Vertical Takeoff Rescue Amphibious Tiltrotor Firefighting Transport (V.T. R.A.F.T) has been under my supervision since the start of the project in mid October. This team has worked hard, and has designed an innovative concept for amphibious tiltrotor operations. The team has used many materials including text books, NASA papers and AIAA papers. All material from these sources is properly cited in this publication. Furthermore I certify that the ideas, concepts, and results presented in this document are original, and have not been plagiarized.

William H. Mason 5-5-2010

Table of Contents

1. Introduction and Review of Relevant Literature

A tiltrotor aircraft combines the versatility of a helicopter with the range and performance of a turboprop. This report proposes an amphibious tiltrotor aircraft for firefighting and rescue operations.

The requirements for the design were specified by the National Aeronautics and Space Administration (NASA) in a Request For Proposal (RFP) posted on www.NASA.gov. The RFP requested designs for a subsonic amphibious tiltrotor aircraft for civilian rescue operations. The aircraft is to land and takeoff vertically from both land and water, including both lakes and oceans, and carry up to 50 passengers. The technical specifications given were a range of 800 nm and a cruise speed of 300 kts. A secondary mission of firefighting was stipulated, necessitating the capability to siphon water into an internal tank and expel it while airborne.

This report describes the preliminary design process of such an aircraft. Three concepts were created and evaluated on mission performance. A conventional tiltrotor design, a quad rotor, and a dual fuselage design were the concepts chosen for analysis. The concepts were evaluated based on aerodynamics, structures, propulsion, performance, stability and control, weight, cost, and mission effectiveness.

The unique mission requirements of V.T. R.A.F.T. mandate a hybrid of many different current aircraft designs, including: seaplanes, aerial firefighting planes, and tiltrotors. From research done by Glenn Curtiss it was determined that water stability would be a driving design constraint, and that a step would be necessary for horizontal takeoff on water. [(1)] John Houbolt's paper on twin fuselage aircraft described the benefits of two fuselages, primarily that the maximum bending moment along the wing is lower. [(2)] Boeing's V-22 pocket guide, and V-22 Information Publication laid out the general design of the systems in a tiltrotor. [(3)] Romander's analysis of NASA's Large Civilaian Tiltrotor influenced the design of the proprotors by describing and analyzing thinning blade theory. [(4)]

2. Discussion of Issues Addressed by the Proposed Design

The V.T. R.A.F.T. is an innovative design that satisfies the RFP requirements, and addresses a number of associated issues. Operational issues that were encountered were the layout of the cabin, the method and equipment used for rescue operations, and the equipment necessary for firefighting. The cabin was designed to either carry the required number of passengers or cargo. The best suited firefighting system for this project is an onboard system, mounted in the floor space under the cabin. Rescue operations may be conducted from either fuselage; each fuselage is equipped with a rescue winch as well as medical equipment.

Aerodynamic issues that were addressed were the design of a wing with an acceptable lift to drag ratio. The aircraft was designed to be capable of sustaining landing loads on both water and land. The wing was designed to support two 4,500 lb wing tip mounted engines, as well minimize the wingtip deflection to accommodate the stiff cross shaft in the wing and minimize aeroelastic effects. Another structural issue that was considered was vibration in the wing, which was most prevalent in transition. This was mitigated by stiffening the wing. Transition was dealt with by using a triple redundant control system. A light yet powerful engine was employed, with a nacelle that was capable of sea operations. The use of a step was deemed unnecessary as the added drag from the step outweighed the benefits of a horizontal takeoff in water. Water stability was addressed by two fuselages so that V.T.R.A.F.T is inherently stable in water.

2.1 History

2.1.1 Seaplanes

The design must be able to land on any body of water. This requires that the hulls of the concepts be able to effectively land, takeoff and maneuver in the water, much like conventional seaplanes. A notable historical seaplane is the PBY Catalina, a multi-role aircraft used heavily between 1930 and 1940. During World War II, it was primarily used for air-sea rescue, anti-submarine warfare, escort, and transport roles. Its ability to land anywhere on the water allowed it to excel in naval operations. [(1)] The Catalina hull featured a step along the bottom of the fuselage approximately 40 feet from the nose. It was determined that this step was necessary from the research done by Glenn Curtiss. He found that no matter how much power a seaplane had, a flat bottom craft would never be able to break free of the water's surface. Unfortunately, the step adds drag in flight due to the shed vortices. [(5)] A tiltrotor can overcome the need for a step by taking off vertically, although this eliminates the possibility of performing a short takeoff on water.

2.1.2 Conventional Tiltrotors

The principle example of a modern tiltrotor is the V-22. The V-22 is a military transport and multi-role tiltrotor first flown in 1989, and has undergone many revisions and improvements over the last two decades. A similar modern design is the Bell/Augusta BA609, a corporate transport tiltrotor. The RFP specifies that the aircraft must be able to land on water; however there exists no such tiltrotor aircraft with that capability to date. Despite this, the V-22 has very similar characteristics to the RFP requirements in payload weight, range and speed. Modern day tiltrotors require a heavily computer augmented control system; this would need to be incorporated in the concept.

2.1.3 Quad Rotors

A solution to the high thrust requirements of tiltrotor aircraft is to increase the number of engines. Quad rotor aircraft have four engines, two forward and two aft of the center of gravity. This design has the advantage of being relatively stable and forgiving of large fore and aft center of gravity movements. The most notable quad rotor was the Curtiss-Wright X-19 developed in the 1960's. This experimental aircraft used two turboshaft engines and was manned by a crew of two. The aircraft had a range of 282 nm and top speed of over 390 kts, significantly faster than conventional tiltrotors. [6] The quad rotor does have the disadvantage of smaller, and therefore less efficient, rotors. In addition, the extra engines can increase the weight of a quad rotor design.

2.1.4 Dual Fuselage Aircraft

There are some advantages in an aircraft having more than one fuselage. In 1982 John C. Houbolt from the NASA Langley Research Center published a paper discussing the advantages of such a design. [2] The paper concluded that a dual fuselage aircraft would reduce the aerodynamic loading on the wing and would require lower amounts of spar material than a single fuselage design. In addition, the dual fuselage would have a lower takeoff gross weight and lower thrust required for flight over a similar design. Despite this, to date, most dual fuselage aircraft have been built to satisfy an unusual design constraint. The Scaled Composites White Knight series of aircraft possess a dual fuselage in order to carry the Space Ship One craft along the aircraft's centerline. Another example is the F-82 Twin Mustang, which was created to provide more fuel space and thus enhance the range of the traditional P-51 Mustang.

3. Detailed Design Specification

3.1 Mission Profile

The mission profile used to assess the concepts was a rescue mission, which was based on the required range of 800 nm and a payload of 50 passengers. The alternate mission was a firefighting mission, where the range was considerably shorter and less design dependent than the rescue mission. For this reason, the rescue mission was chosen as the design constraint for the aircraft. During the rescue mission, the aircraft performs a vertical takeoff, climbs vertically to an altitude of 600 ft, transitions to forward flight, then climbs to 10,000ft where it cruises for 400 nm, it then descends to 600 ft, converts back to helicopter mode and lands vertically. After landing on land or water, the passengers are loaded and the aircraft returns using the same flight path.

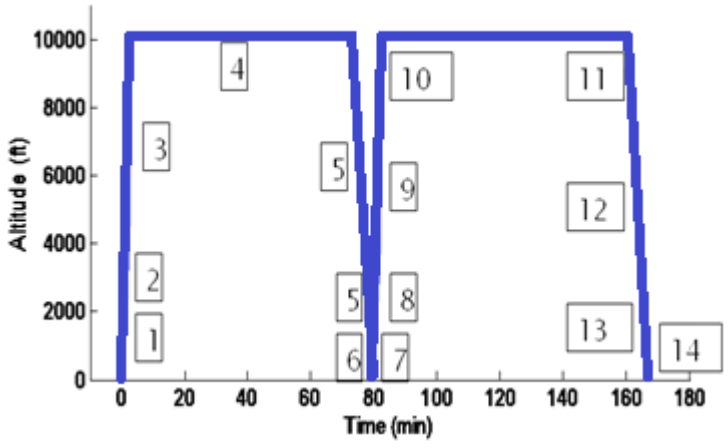

1	Vertical Takeoff (2100ft/min)
2	Transition(30sec)
3	Climb
4	Cruise
5	Glide down
6	Conversion
7	Landing
8	Vertical Takeoff (2100ft/min)
9	Transition
10	Climb
11	Cruise
12	Glide down
13	Conversion
14	Landing

Figure 3.1.1 Mission Profile

3.2 Conventional Tiltrotor Concept

Based largely on the V-22, the single fuselage, two-nacelle design concept was developed as a simple, conventional solution to the RFP. However, the RFP requires twice the passenger capacity and a cruise speed that is about 40 kts faster than the V-22. With these requirements, it was concluded that a larger aircraft with respect to volume and weight was needed.

The V-22 was limited in rotor size and wingspan by the need to be stored on a carrier deck; however this is not a constraint for this concept. Thus, the rotors are larger than the V-22 rotors to improve vertical takeoff performance. Twelve foot long wingtip extensions were added to the engines to increase the wingspan and increase lift to drag ratio in cruise. The wingtip extensions rotate with the engines to minimize downwash during vertical takeoff.

To account for the extra passengers, the conventional concept possesses a more rounded fuselage with a larger inner diameter and a greater length than the V-22. The greater internal volume is utilized by adding a removable center row that effectively doubles the number of seats available for passengers. There are two doors located on either side of the fuselage for loading and unloading passengers and cargo. There are also rescue winches mounted at each door for aerial rescue.

The base of the fuselage was adapted for water landings. The fuselage was designed to resemble a boat hull with a step located at 18° off of the center of gravity and a stern post angle of 7°. The sea hull design was based on the design of a seaplane found in Raymer. [7] Even with the sea hull design the conventional concept was deemed extremely unstable in any sea state. This necessitated pontoons near the wing tips. The pontoons were considered a negative factor due to the added complexity, structural weight and increase in drag due to aerodynamic interference.

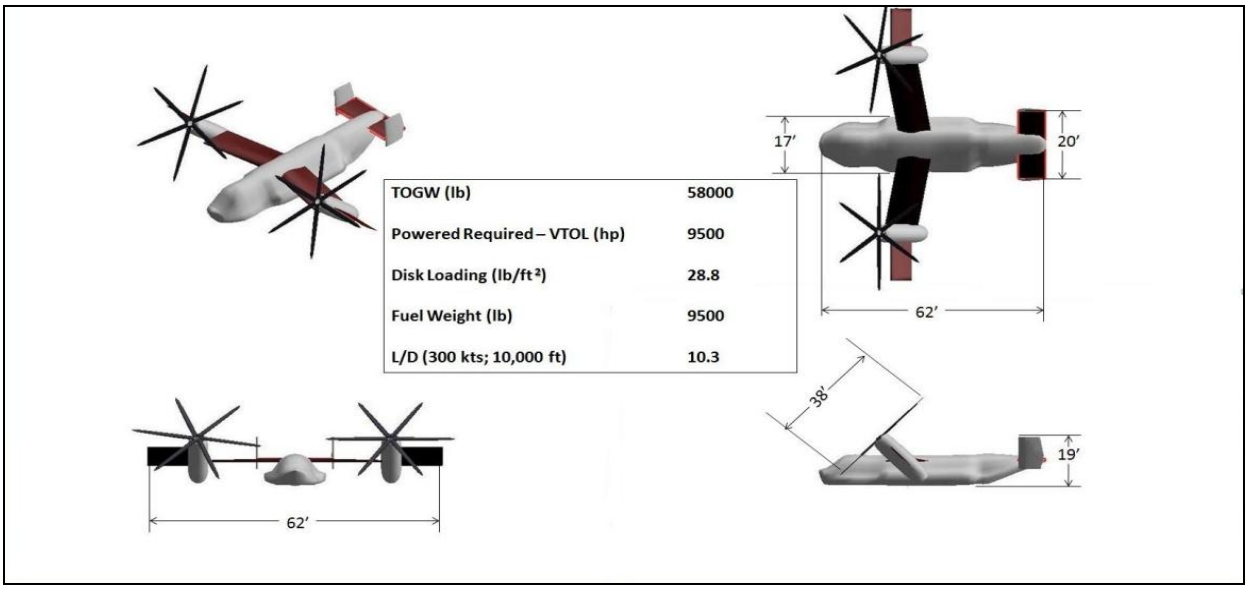

TOGW (lb)	58000
Powered Required – VTOL (hp)	9500
Disk Loading (lb/ft²)	28.8
Fuel Weight (lb)	9500
L/D (300 kts; 10,000 ft)	10.3

Figure 3.2.1 Conventional Concept (Pontoons not pictured)

3.3 Quad Rotor Concept

A quad rotor design was originally developed to achieve the required cruise speed and to satisfy the vertical takeoff thrust requirement through the use of four engines. The initial design for the quad rotor was heavily influenced by historical experimental craft such as the X-19. One significant difference between historical quad rotors and this design is the addition of a 15 ft vertical tail. Quad rotors have an extremely complex stability and flight control system, even compared to an already complicated conventional tiltrotor. Traditionally, the use of large, heavy, and complex gear boxes were used to generate variable propeller speeds between cross-shafted rotors to control the yaw. The historical failure rate, weight, and complexity of these gearboxes were minimized through the inclusion of a vertical tail for yaw control and added stability. [6]

Another key design feature of the quad rotor concept is the vertical offset and different sizing of the two wings. This was present in the X-19, and was included in the current concept for better aerodynamic characteristics. The front wing has a span of 65 ft with an aspect ratio of 6.8, while the rear wing has a 76 ft span with a 9.5 aspect ratio. By having a larger span on the rear wing, it allows the propeller wash of the front rotors to not degrade the airflow to the rear rotors. The fuselage of the quad rotor is identical to that of the conventional concept.

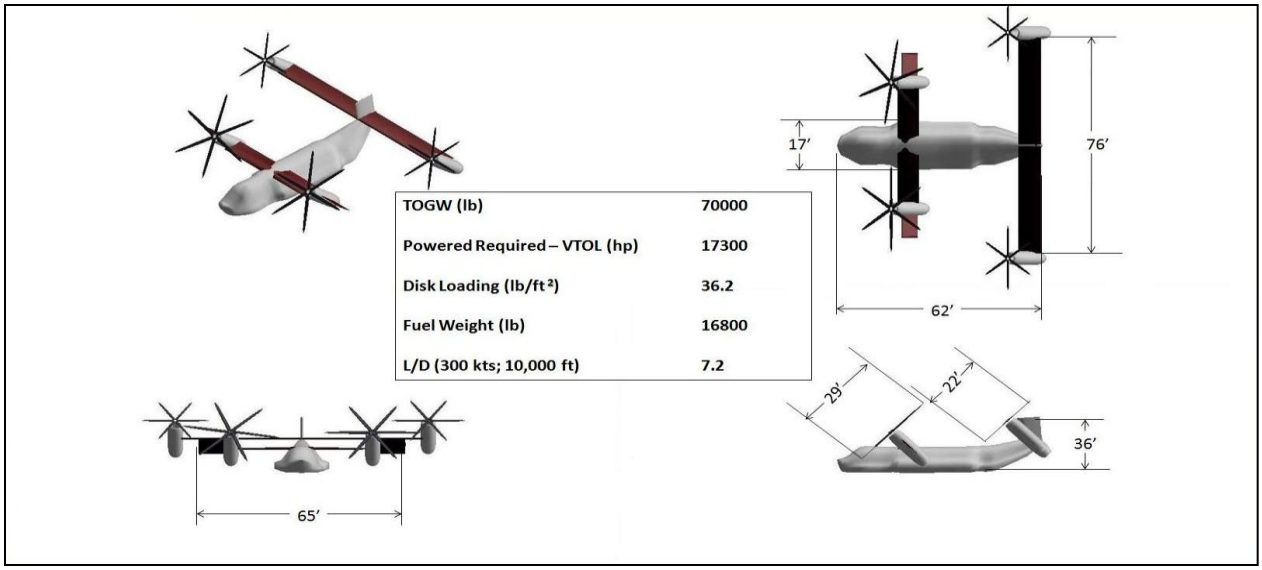

Figure 3.3.1 Quad Rotor Concept (Pontoons not pictured)

3.4 Dual Fuselage Concept

A significant issue encountered during amphibious operations is stability while on the water. A traditional single fuselage design will tend to roll over onto a wingtip while powered off on the water, and thus requires a large pontoon system. If the pontoon is not retractable it will incur a large amount of drag, and if the pontoon does retract, it will necessitate a complex and heavy retraction system. To mitigate these water stability problems, a dual fuselage concept was proposed.

The dual fuselage concept has a high, straight wing with two fuselages suspended equidistant from the center of the wing. Each fuselage has a vertical stabilizer, which is connected by a single horizontal stabilizer. The outboard wings are the same length and aspect ratio as the wings on the conventional concept, and the rotors are the same size as the conventional concept's rotors.

Each fuselage contains seats for half of the passengers. In the rear of each fuselage, there is a rescue door, facing towards the other fuselage. By placing the rescue doors on the inside of each fuselage, passengers can be loaded between the fuselages, out of the downwash of the rotors. The cockpit is located in the left fuselage. Concept Evaluation and Decision

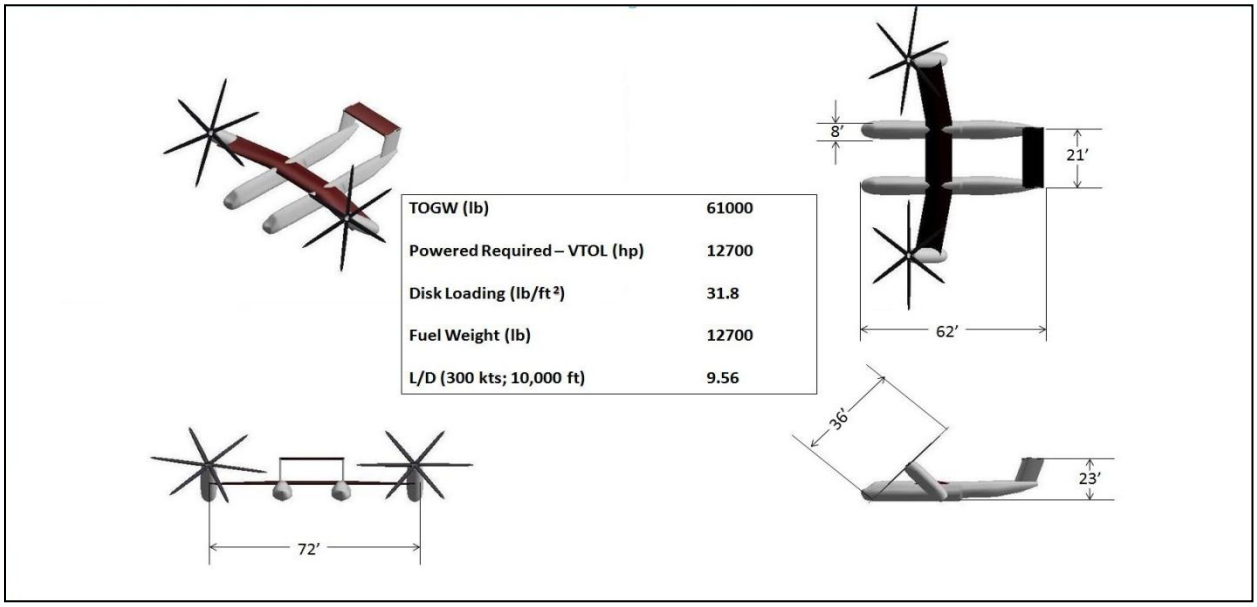

Figure 3.4.1 Dual Fuselage Concept

3.5 Decision Process

3.5.1 Quantitative Decision Matrix

The characteristics of each concept that were evaluated quantitatively were placed in a decision matrix. The most important characteristic was power required for vertical takeoff, as this drives the engine and rotor size. Lift to drag ratio in cruise at 10,000 ft and 300 kts was considered the next most important characteristic, as this value determines the range and fuel efficiency of the aircraft. The fuel weight, disk loading, maximum bending moment, and center of gravity movement were also included in the matrix, in that order of importance. Gross takeoff weight was not included directly in the matrix, as the weight is already reflected in other parameters, especially power required. Including takeoff weight as a separate category would have counted its importance twice.

For each value in the matrix, the best performing aircraft was given a score of 1, and the other aircraft were normalized to that value. For example, the conventional concept had the most favorable cruise *L/D*, 10.3, while the dual fuselage had an L/D of 9.56. Thus, the conventional L/D score was set to 1, and the dual fuselage score was set to 10.3/9.56, or 1.02. The entire quantitative matrix can be seen in Table 3.4.1

It can be seen in Table 3.5.1 that in every aspect except for center of gravity movement the conventional design performed the best. The dual fuselage obtained scores close to the conventional in all categories, while the quad rotor concept was far inferior to the other two concepts.

Table 3.5.1 Quantitative Design Matrix

	Weight	Quad Rotor	Dual Fuselage	Conventional
Power Required (VTOL)	8	1.82	1.16	1
L/D (Cruise @ 10,000 ft)	7	1.41	1.07	1
Fuel Weight	6	2.1	1.11	1
Disk Loading	5	2.52	1.1	1
Max Bending Moment	4	1.15	1.09	1
CG movement	3	1	2	2
TOTAL		**57.23**	**39.29**	**36**

3.5.2 Qualitative Decision Matrix

Table 3.5.2 shows the qualitative decision matrix that was used to evaluate the three conceptual designs. The desired qualitative traits for an aircraft meeting the RFP are ease of operation, water stability, less system complexity, lower maintenance costs, and a long service life. Importance rankings for each of the aforementioned traits are listed in Table 3.5.2, with 1 being the most important and 4 being the least. The associated weights of each qualitative category are listed in the second column of Table 3.5.2. A ranking system of 1 through 3 was used in determining how well each concept met the qualitative categories with 1 being the best and 3 being the worst.

Water stability was determined to be the most important qualitative trait for an aircraft meeting the RFP because it is the only qualitative trait required by the RFP. The dual fuselage is the only concept that is inherently stable on water because the aircraft's center of gravity is balanced between two contact points with the water. Both the quad-rotor and conventional concepts would tip over on water unless an additional pontoon system was added. A pontoon system would increase the system complexity, weight, and drag of the concepts. The dual fuselage therefore obtained the highest rank in the water stability category whereas the quad rotor and conventional concepts obtained the lowest rank.

Table 3.5.2 Qualitative Design Matrix

	Weight	Quad-Rotor	Dual Fuselage	Conventional
Ease of operation	6	2	3	1
Water stability	12	3	1	3
Rescue Operations	8	3	1	2
System complexity	6	3	1	1
Maintenance	4	3	2	1
Service Life	3	3	1	2
TOTAL		**111**	**55**	**74**
OVERALL TOTAL		**168.23**	**94.29**	**110**

The second most important qualitative trait for the aircraft meeting the RFP is the ease of conducting rescue operations. The dual fuselage concept is the best at conducting rescue operations because it is the only concept capable of using a winch system from both rear and side loading doors in rescue operations. This is because the region between the two fuselages does not experience the downwash caused by the rotors, so that people can be safely raised up to the inside facing doors of the dual fuselage. If a winch system were included on the conventional or quad rotor concepts, the winches would have to be placed underneath the downwash of the rotors because that is where the fuselage doors are located.

Ease of operation, system complexity, maintenance, and service life were of lesser importance than water stability because none were specified by the RFP. The quad-rotor and dual fuselage concepts received lower rankings than the conventional concept in the ease of operation category because the quad rotor has two more tiltrotors to manage than the conventional, and the dual fuselage concept would have more difficulty landing in smaller areas than the conventional concept. Both the dual fuselage and conventional concepts received higher rankings for system complexity because they both have to control two rotors as opposed to the four rotors. The

conventional concept was determined to have the lowest required maintenance because it has the lowest number of components to maintain. For instance, on the dual fuselage concept the rust build up on both fuselages due to water landings has to be maintained, and on the quad rotor concept four engines have to be maintained instead of two. The dual fuselage concept received the highest rank in service life, because it experiences the smallest wing bending moment in cruise, thus reducing the overall fatigue of the wing and reducing crack propagation.

3.5.3 Final Decision

It was decided that the dual fuselage was the best design based on the specified RFP, and the calculated data. Quantitatively the performance characteristics of the conventional and the dual fuselage concepts were very similar. The relative cost for the conventional and the dual fuselage concepts are comparable. However, mission completion was the most important aspect of the decision and the dual fuselage significantly outperforms the other concepts in this category. More specifically, the dual fuselage had much better water stability characteristics than the conventional and quad rotor concepts.

Another requirement of the mission is the ability to rescue individuals in disaster type situations. By having two fuselages there were twice as many entrances than there were on the conventional concept, this allows people to enter and leave twice as fast. In addition, with two fuselages the area in between the fuselages is protected from the downwash of the rotors, allows for rescue winches to be placed on the interior doors to be used for air-land rescue operations. This cannot be accomplished in the conventional design as the downwash from the rotors makes the rescue winch cable unsteady and unreliable.

Like any aircraft, the dual fuselage will require routine maintenance. By having two fuselages the dual fuselage concept will have more volume to place components than the conventional concept. This added volume will make it easier to access components that wear out over time.

3.6 Overview and General Sizing

The V.T. R.A.F.T. concept was designed to fulfill the requirements specified in the RFP. It has a wing span of 76.5 ft and is 60 ft in length with a gross takeoff weight of 62,460 lb. Wing size was obtained through a tradeoff between structural weight and aerodynamic characteristics; additionally, fuselage size was determined by requirements for passenger volume. The aircraft is capable of performing an amphibious vertical takeoff with 50 passengers or 12,000 lb of water and cruises at 300 kts. This makes the aircraft ideal for rescue and firefighting applications. In addition, the aircraft is designed to perform a short takeoff with an increased gross weight of 70,000 lb. This enables the aircraft to increase the payload carried by approximately 60%. Design and analysis of the aircraft is detailed Sections 3.6 – 3.13.

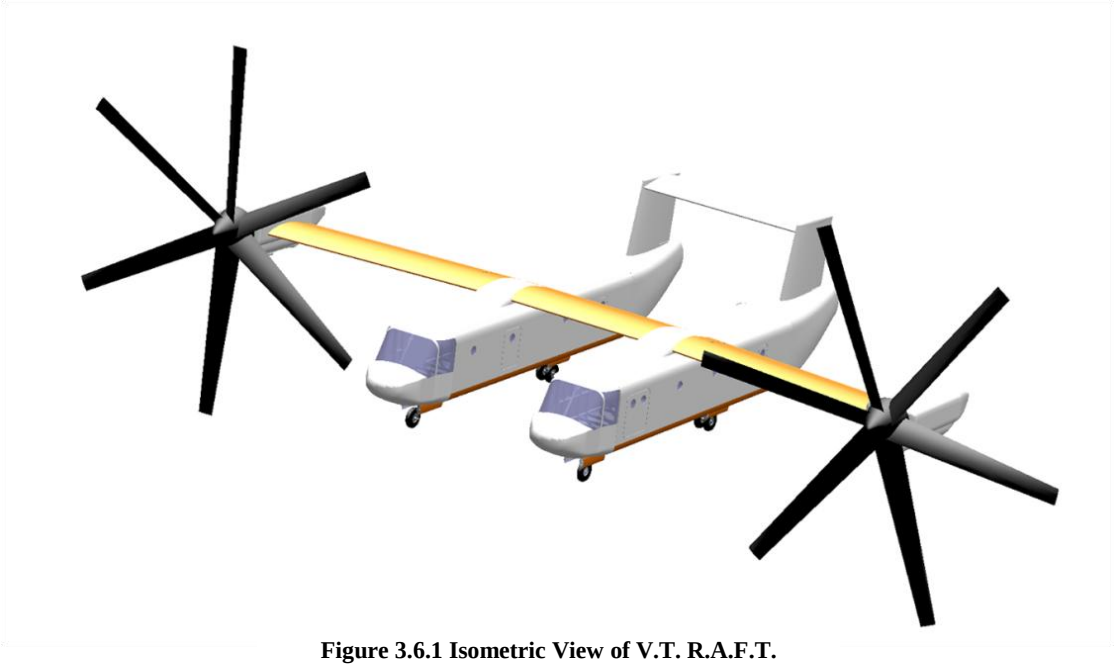

Figure 3.6.1 Isometric View of V.T. R.A.F.T.

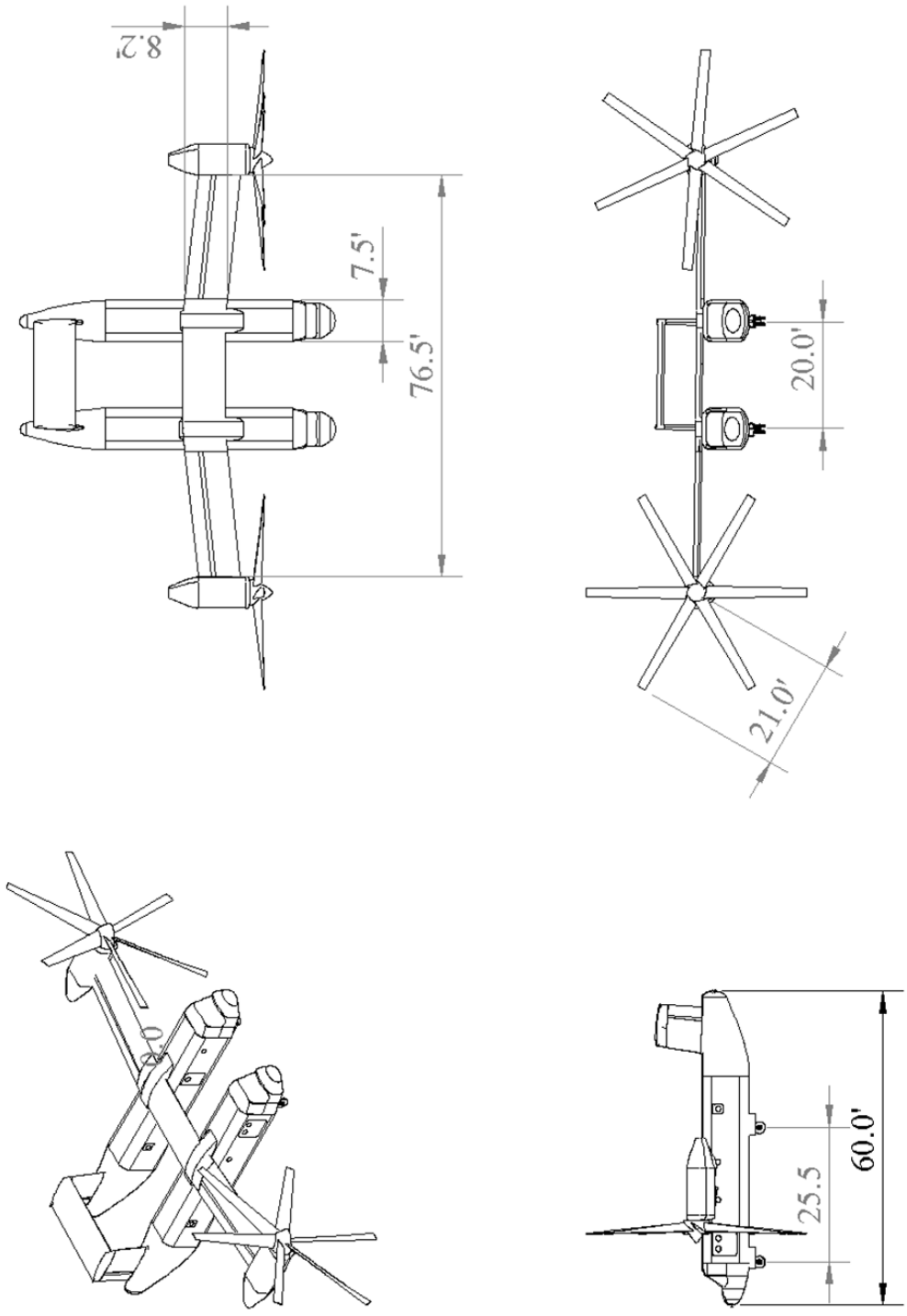

Figure 3.6.2 Three View and Isometric View of V.T. R.A.F.T.

3.7 Weight Estimation

A large components method outlined in Chapter 15 of Raymer was used for preliminary design. The method uses statistic data of similar aircraft and the wetted areas of the major components. The payload was determined to be 200 lb for each of the 50 passengers and 6 crew members and 500 lb for medical equipment. This yielded a payload weight of 11,700 lb and a fuel weight of 12,000 lb; the TOGW was estimated to be 63,740 lb. This weight was used for sizing and other major preliminary design decisions.

The final weight estimation was determined by summing the weights of the actual structural components and aircraft systems. The weights of the individual components were determined by modeling the parts in Solidworks and specifying a material density. Using the same payload and fuel weight specified before, the final TOGW is 62,460 lb. The detailed weight estimation table can be seen in Appendix A.

3.8 Propulsion

A tiltrotor aircraft requires a unique propulsion system that must adequately perform in both Vertical Takeoff and Landing (VTOL) and conventional airplane mode. The RFP mission requirements and the tiltrotor design limitations cause many limiting factors in a propulsion system. The propulsion system selected must be able to provide adequate thrust in VTOL operations with a safe and acceptable vertical climb rate. The propulsion system must also be able to meet the RFP requirements and be able to obtain a 300 kts cruise speed at cruise altitude (10,000 ft). After preliminary analysis and research, the propulsion system was designed around a mission profile consisting of vertical takeoff and landing at sea level assuming the aircraft was out of ground-effect as it is a more stringent condition.

3.8.1 Engine

The engine selection for a tiltrotor is limited. Historically, turboprop and turboshaft engines have been used in tiltrotor aircraft. For the V.T. R.A.F.T. project, an existing engine was desired to allow for ease of production and reduction in cost. A turboshaft engine was chosen over a turboprop because of the turboshaft's ability to provide larger amounts of shaft horsepower. The selection of a turboshaft engine is consistent with current production tiltrotors such as the V-22 and the Bell/Augusta BA609. As a result of these selection criteria, the Rolls Royce AE 1107C Liberty engine was chosen for this design. The AE 1107C is specifically designed to power tiltrotor aircraft. It provides 6150 shp and has been proven in over 17 million hours of operation. Many of the AE 1107C's components are shared with other Rolls-Royce engines and are therefore a more maintainable engine over a newer design. The engine is designed for high efficiency operation and consists of a 14-stage compressor as well as a two stage gas generator and power turbine. A unique feature of the engine is a self-contained oil system that lubricates the engine and is designed for efficient vertical flight. The AE 1107C provides an off the shelf power option that is designed for tiltrotor operations and can more than effectively meet the requirements of the V.T. R.A.F.T. design. [8]

Figure 3.8.1 Rolls Royce AE 1107C Liberty Engine [8]

3.8.2 Proprotor

As encountered with other aspects of the propulsion system, the design of the proprotor also had to accommodate both VTOL and horizontal flight. In addition, the high cruise speed required in the RFP and the large power/ thrust requirement for VTOL requires a redesign of current blade configurations. The first step in designing the proprotor was to determine its diameter. A large proprotor diameter was sought to allow for large thrust production in VTOL, a lower proprotor rpm and a lower tip speed when compared to a smaller diameter rotor. Upon consultation with both structures and aerodynamic teams, it was determined that a proprotor with a radius of 21 ft was the largest possible proprotor radius that allowed for safe clearance from the fuselages. The airfoils used in the proprotor design are XN series airfoils, which are specifically designed for tiltrotor operations. The XN airfoil series is also used on the V-22 proprotor. Due to the stress placed upon the proprotor, particularly at the root in VTOL, a large root thickness is required. For best propulsive characteristics in conventional flight, narrower blades are desired. For this reason, the blade design uses five XN airfoil sections to allow for greater strength near the rotor hub while providing an efficient design at the tip of the rotor. The 300 kts cruise speed was a limiting factor in rotor

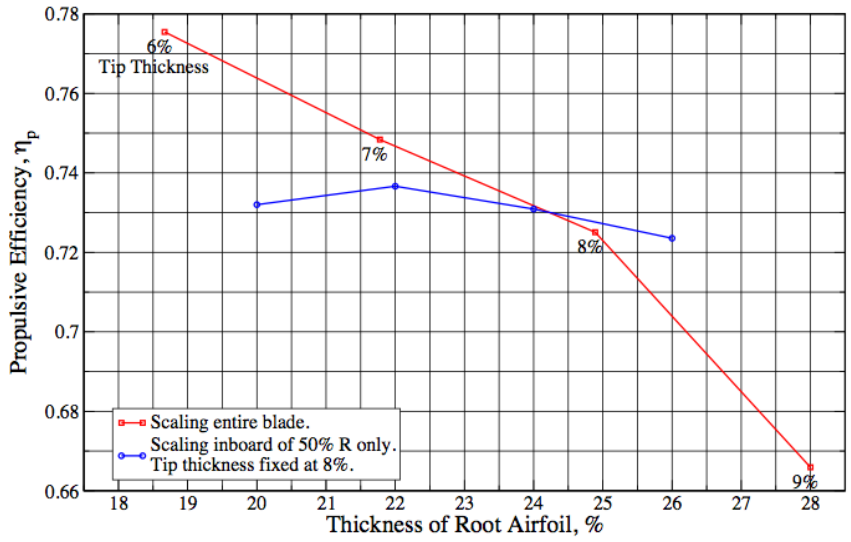

Figure 3.8.2 Effect of rotor thinning on propulsive efficiency [4]

design because current production tiltrotors do not reach such high cruise speeds. The solution to this problem was found by NASA through work on the Large Civilian Tiltrotor. Ethan Romander at NASA Ames used 3-D Navier- Stokes Analysis and blade thinning to find a blade that could reach a 350 kts cruise speed. From Romander's analysis, it was found that using a constantly thinned blade from root to tip with a tip thickness of 6% increased the propulsive efficiency of the rotor from 66% to 78% as shown in Figure 3.8.2. [4]

With this analysis in mind, the rotor was designed using five thinned XN airfoils (the number in the XN designation corresponds to the maximum thickness) shown in Table 3.8.1.

This thinned rotor uses a 25% thickness XN airfoil at the root to accommodate the stresses on the rotor, and gradually thins out to a 6% thickness at the root to reach 78% efficiency. The tip of the rotor is a progressive sweep tip that allows the rotor tip to reach speeds of Mach 0.8. [9] The rotor has a 39° angle of twist (-48° Inboard/-30° Outboard) and has a constant chord of 2.97 ft. [4] The rotor blade itself is manufactured of a high strength rigid composite fiber material and has a thin titanium – alloy anti-abrasion strip on the leading edge for durability. [3] The number of blades per each proprotor was determined by first finding the tip speed ratio to be 1.778. From this number, it was determined that a seven bladed proprotor would provide optimal performance [9]; however, using a six bladed rotor provided a large weight reduction with negligible performance losses; therefore, a six bladed proprotor was chosen.

Table 3.8.1 Rotor airfoil sections and positions as fraction of rotor length

Airfoil	r/R
XN25	0.06
XN18	0.12
XN12	0.5
XN08	0.75
XN06	0.99

3.8.3 Gearbox and Cross Shaft

The propulsion system uses five gearboxes to efficiently accomplish all aspects of the propulsion envelope desired in tiltrotor operations. The engines each have swashplates much like those needed in helicopters, controlling the angle of attack of each rotor blade. A proprotor gearbox (PRGB) provides mounting for the proprotor on the nacelle and uses speed reduction to allow the proprotor to spin at 297 rpm while the engine spins at 15000 rpm, under normal operating conditions. The tilt-axis gearbox (TAGB) allows for the rotation of the nacelles and for the transmission of power to the cross shaft and auxiliary power unit. Lastly, one gearbox is placed in the left fuselage and acts as a gearbox for the auxiliary power unit (APU). The APU gearbox (APUGB) is connected to the cross shafts coming from either nacelle and allows the APU to power necessary aircraft systems without the engines running. The most important aspect of the APU gearbox is that in the event of an engine out situation, it transfers power from the working engine across the cross shaft to the non-working engine's proprotor to allow for one engine emergency operation. [10] Each outboard wing has four 7 ft cross shaft sections and the inner wing has three 6 ft sections. Each section is joined by a coupling that allows for a 5^0 bend. All gearboxes are assumed to be highly efficient with losses of less than 3%.

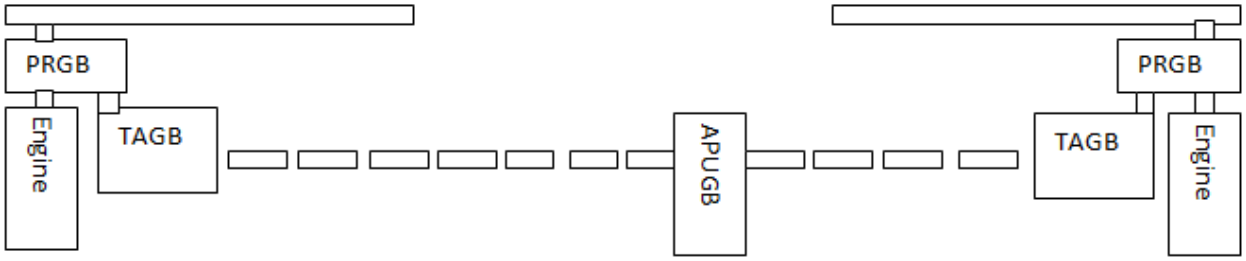

Figure 3.8.3 Gearbox and Cross Shaft Diagram (Not to scale)

3.8.4 Performance Characteristics

Through careful rotor design and engine selection, a propulsion system that excels in both VTOL and conventional performance was designed. In VTOL mode, the V.T. R.A.F.T. has the propulsive characteristics shown in Table 3.8.2. At maximum power and normal sea level conditions, 77050 lb of thrust are produced. In VTOL operations the thrust is reduced to 69350 lb due to a 10% downwash on the wing. In a propeller type operation, the proprotor has an efficiency of 0.78 and can propel the aircraft over 330 kts at sea level.

Table 3.8.2 Proprotor Characteristics

Disk Loading	21.98 lb/ft^2
Solidity	0.270
Figure of Merit	0.810
Coeff. Of Thrust	0.029

3.8.5 Nacelle Design

The nacelle design is based on the V-22 nacelle, which is designed for ease of maintenance. The nacelle is slightly smaller to account for the lack of an infrared suppressor. The intake is designed to reduce foreign object digestion into the engine. A particle separator is located just past the inlet and is designed to remove particles 20 microns in size and larger. [3]

A unique problem associated with the amphibious operation of a tiltrotor is that the engine exhaust has the potential to be submerged in the water. Currently, there is 1.5 ft of clearance in standing water between the nacelle and the water surface. To ensure that the exhaust is not submerged in higher sea states, an exhaust rerouting system was developed. The system uses a series of valves that when activated, reroute the engine exhaust to the side of the nacelle. At the same time, the rear of the engine nacelle is sealed, allowing it to be submerged without affecting the engine performance. The reroute system is activated only in VTOL operations where the aircraft is actually floating on the water's surface.

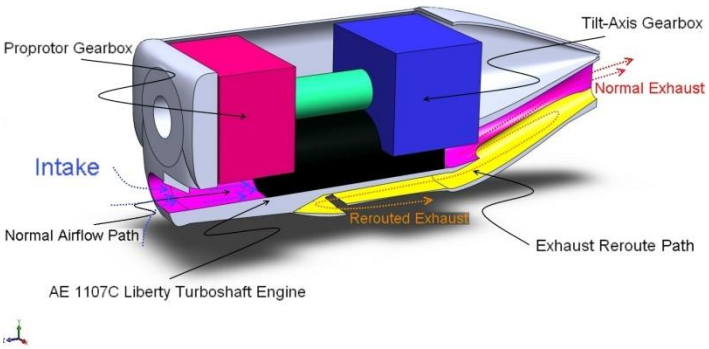

Figure 3.8.4 Nacelle Design

3.9 Aerodynamics

3.9.1 Goals and Requirements

The 800 nm range requirement and the transition between vertical and horizontal flight modes were the driving aerodynamic considerations for the design. To achieve the range requirement it was imperative that drag be reduced as much as possible and a high lift to drag ratio (*L/D*) achieved. The higher this ratio, the less fuel the aircraft requires, which in turn eases vertical takeoff and reduces engine weight.

To achieve a high *L/D*, the wing should be small but with a large wingspan. The airfoil should also have a high coefficient of lift (C_l) at zero degrees angle of attack, to eliminate the need for wing incidence. It was considered acceptable for the airfoil to have a zero angle of attack C_l of 0.3 or greater. In addition, the fuselage must prevent flow separation, as this creates pressure dag which can dramatically decrease *L/D*.

The transition between flight modes requires the aircraft to fly slowly without stalling. This heavily influenced the airfoil selection; when choosing airfoils for the main wing it was considered necessary for the airfoil to have a stall angle of attack of over 12° at Reynolds numbers no higher than 4 million. Furthermore, the airfoil chosen for both the inboard and outboard wings must have a high thickness to chord ratio; in tiltrotor applications a thin wing will be very prone to wing flutter. To mitigate flutter, the thickness to chord ratio must be at least 0.15.

3.9.2 Airfoil Selection

The NACA 65(216)-415 a=0.5 airfoil was selected for both the inboard and outboard wing sections. The airfoil has a stall angle of attack of 15° for Reynolds numbers above 3.1 x 10^6. This satisfies the requirement for low speed transition performance. The airfoil's thickness to chord ratio of 0.15 is sufficient to mitigate wing flutter. In addition, the airfoil possesses a zero degree angle of attack C_l of 0.3, which is high enough to allow cruise at zero degrees angle of attack. At this C_l the airfoil promotes laminar flow over the wing, which makes it an ideal choice for the center wing.

3.9.3 Wing Geometry

When cruising at 300 kts, minimal drag occurs at the airfoil's design C_L of 0.4. From this constraint, as well as the aircraft's weight and cruise velocity, the optimal wing area was calculated to be 625 ft^2.

The wing span was then varied so that *L/D* could be maximized. The Torenbeek wing weight equation for heavy transport aircraft [11] was incorporated with the drag estimation methods detailed in section 10.4 to determine the aircraft's lift to drag ratio (*L/D*) versus wingspan. The wingspan was chosen to be 76.5 ft as a compromise between aerodynamics and structural considerations. This wingspan led to a chord of 8.2 ft. The plot of cruise *L/D* versus wingspan may be seen in Figure 3.9.1.

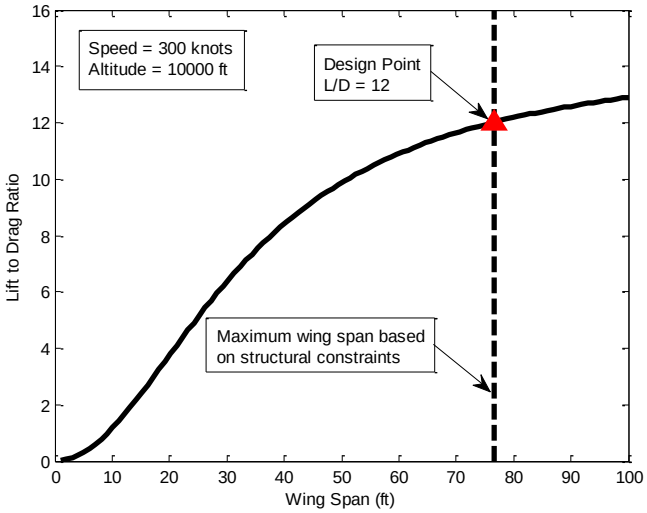

Figure 3.9.1 Lift to drag ratio as a function of wingspan, using fixed wing area and Torenbeek wing weight model [11]

3.9.4 Fuselage Geometry

A chief concern for the shape of fuselage was whether to include a rear loading door similar to that on the V-22. The inclusion of a rear loading door would allow for easier loading of the aircraft with medical cargo and palettes that would increase the water storage capacity of the aircraft. However the sharp angle that the retracted rear loading door would make from the flow over the fuselage would cause boundary layer separation and a 60% in drag. The large increase in drag provided enough justification to discard the idea of including a rear loading door.

3.9.5 Drag Estimation and *L/D*

3.9.5.1 Cruise Drag Estimation Methods

The aerodynamic drag acting on the aircraft in cruise was estimated using two different approaches. For the first approach the skin friction drag and induced drag was calculated using several custom programmed MatLab files. In the second approach a program supplied by Dr. Ohad Gur was used to evaluate the drag [12]. The *L/D* values calculated by both drag models were approximately the same. The final *L/D* value for the aircraft is 12, a 25 % increase over the original dual fuselage concept.

3.9.5.2 Custom Drag Estimation Model

The aerodynamic drag force acting on the dual fuselage concept was obtained by calculating the skin friction drag, induced drag, and form factors at cruise conditions. Cruise conditions for the concepts consisted of flying at 300 kts as required by the RFP and at an altitude of 10,000 ft at standard atmospheric conditions. This altitude was chosen because that is the maximum altitude an aircraft can fly before requiring pressurization of the cabin.

Skin friction drag was estimated using the analytical solutions for the boundary layer thickness over a flat plate. The wetted area of the dual fuselage was estimated by calculating the surface area of geometrical objects that best represented the configuration of the aircraft. Each section of the aircraft was decomposed into regions represented by either the shape of a flat plate or a cylinder. The dimensions of cylinders and flat plates representing the aircraft were then used to calculate the surface area and the skin friction coefficient at the trailing edge of each shape. The skin friction coefficient would then be doubled to obtain the average skin friction coefficient acting on that particular shape.

The induced drag was calculated using aircraft performance methods. The weight of the aircraft in cruise was assumed to be the gross takeoff weight so that a conservative value for the induced drag could be calculated. The induced drag coefficient was then calculated using the lift coefficient, the aspect ratio of the aircraft, and an estimated Oswald efficiency factor. The Oswald efficiency factor was estimated to be 0.9 because the location of rotor nacelles on the wing was expected to reduce the span wise flow along the wing and therefore the downwash.

Form factors for the fuselage and wing were calculated using equations in Chapter 12 of Raymer. The form factors were calculated directly from the geometry of the aircraft. These form factors, skin friction coefficients, wetted areas, flow dynamic pressure, and reference areas for each component of the aircraft were used to obtain the overall parasite drag coefficient.

The parasite drag coefficient and the induced drag were added together and multiplied with the dynamic pressure and corresponding reference areas to obtain the total drag force. The total drag force was then used to obtain the lift to drag ratio, thrust required, and power required.

3.9.5.3 Full Configuration Drag Estimation Model

The aerodynamic analysis program provided by Dr. Ohad Gur was used to compute the drag acting on the aircraft so that the custom drag analysis methods could be verified. A geometrical shape for the aircraft had to first be entered into a text file. A compiler would then estimate the drag coefficient for the aircraft shape entered in the text file and also create a Visual Sketch Pad file that showed the physical representation of the aircraft being analyzed. A paper by Dr. Gur gives a rigorous explanation of how the program estimates the drag [12].

The *L/D* value calculated by both the Full Configuration Drag Estimation and the custom drag estimation model was calculated to be about 13. An *L/D* value of 12 was chosen as final for the aircraft because neither drag estimation model calculated the skin friction drag acting on the engine nacelles of the aircraft. The power required as a function of airspeed at cruising altitude can be seen in 3.9.2. Additionally Figure 3.9.3 shows how the *L/D* varies with altitude at cruising speed; demonstrating how the *L/D* of the aircraft improves with altitude up to about 30,000 ft. The higher *L/D* values at higher altitudes motivate the option to include an oxygen system for the crew on the flight to rescue the refugees so that the aircraft obtains improved specific fuel consumption.

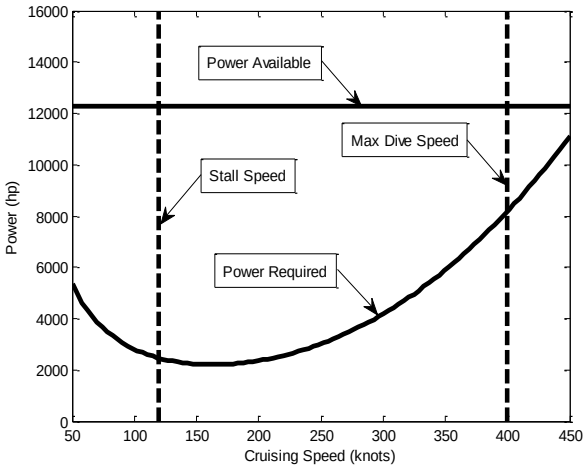

Figure 3.9.2 Power required in forward flight as a function of airspeed

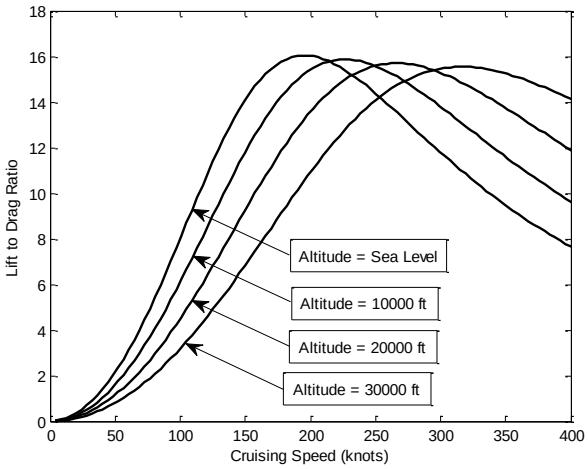

Figure 3.9.3 Plot of L/D as a function of cruising altitude

3.10 Performance

3.10.1 Fuel Weight

The fuel weight for the aircraft was calculated to be 10,175 lb. This includes a 10% reserve and a 5% allowance for climb. The fuel weight was determined by manipulation of the Breguet Range equation into the form of (equation 3.10.1):

$$W_f = \mathrm{W_i} * e^{\frac{-R*C_{power}\ \frac{D}{L}}{\eta_p}} \tag{3.10.1}$$

where R is the range in ft, η_p is the propeller efficiency, C_{power} is the coefficient of power in units of 1/ft, L/D is the lift to drag ratio, $W_{i,}$ is the initial weight in pounds, and W_f is the final weight in pounds. The fuel weight will be the difference between the final and initial weights.

The assumptions made to use this equation were that the initial weight of the aircraft was both the empty weight and the payload, and that the propeller efficiency, η_p, was approximately 0.8. The coefficient of power, C_{power}, (equation 3.10.2) was calculated based on the rotor disk area:

$$C_p = \frac{P*550}{\pi R^2 \rho {V_t}^3} \tag{3.10.2}$$

where P is the shaft horsepower required for cruise flight, ρ is the density of air in which the plane is flying, R is the radius of the rotor in feet, and V_t is the tip speed of the rotor in ft/s.

3.10.2 Short Takeoff

The V-22's ability to perform a short takeoff improves its payload capacity and its mission abilities. It was therefore a plausible option for V.T. R.A.F.T. The short takeoff weight, as determined by the maximum load that can be supported by the wings and fuselage, was determined to be 70,000lb. In order to determine the short takeoff weight the takeoff speed and effective weight had to be calculated. The takeoff speed is typically 15 to 20% of the stall speed of the aircraft. The stall speed is determined by the following (equation 3.10.3):

$$V_{stall} = \sqrt{\frac{2W_{eff}}{\rho S C_L}} \tag{3.10.3}$$

where W_{eff} is the effective weight, ρ is the density of air at sea level, S is the planform area and C_L is the maximum coefficient of lift at zero degrees angle of attack. The effective weight is calculated using the following equation:

$$W_{eff} = W - Tsin(\theta) \tag{3.10.4}$$

where W is the gross takeoff weight, T is the total thrust produced by the engines, and θ is the angle to which the nacelles are rotated measured from the horizontal. With the takeoff velocity and the effective weight the short takeoff distance can be determine using equation (3.10.5)

$$S_{TO} = \left(\frac{W_{eff}}{g\rho S\,(C_d - \mu C_l)}\right) \ln\left(\frac{\frac{T_0}{W_{eff}} - \mu}{\left(\frac{T_0}{W_{eff}} - \mu\right) - \left(\frac{1}{2W_{eff}}\right)\rho S\,(C_d - \mu C_l)}\right) \tag{3.10.5}$$ [13]

where T_0 is the horizontal portion of the thrust due to the engines, μ is the coefficient of friction which is assumed to be 0.02 (smooth surface), and C_d is the coefficient of drag. The short takeoff velocity was determined to be 72 kts and the short takeoff distance was approximately 42 ft.

3.11 Stability and Control

Tiltrotor aircraft have more complex stability and control requirements than conventional aircraft. The requirements for a tiltrotor can be divided into two phases: vertical flight and cruising flight. In vertical flight the aircraft is required to be stable without the use of a tail. Due to the lack of an ability to generate a pitching moment, the center of gravity must be very close to the center of lift to maintain stability. Control requirements in vertical flight are not a driving constraint as the rotors can be tilted to provide large amounts of thrust to perform any hover maneuver. In horizontal flight dynamic stability was required. Control requirements for the aircraft were based on

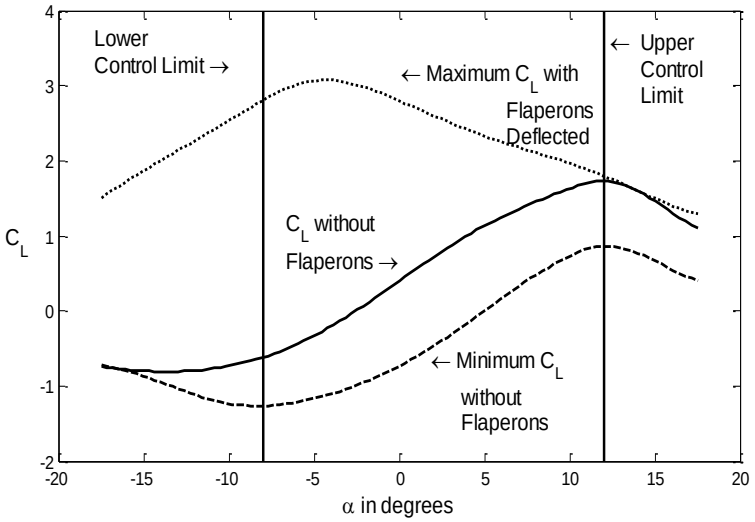

Figure 3.11.1 Lift coefficient values as a function of angle of attack, with and without deployment of flaperons.

existing V-22 control capabilities. These included a pitch rate of 6°/sec per in of stick, and roll and yaw rates of 4°/sec per in of stick, with a maximum stick deflection of 6 in.

The control configuration in vertical flight consists of rotating the nacelles to a position that will provide adequate thrust to lift the vehicle. In addition, there are flaps that can be deflected to minimize the wing reference area, and thus the downwash on the wing. The control configuration in cruising flight is the classical aerodynamic control scheme consisting of a rudder, ailerons, and the elevator.

Vertical flight requirements drive the size of the flaps because in vertical flight approximately 12.5% of the downward thrust is lost on the wing. To reduce this, flaps that are 35% of the chord were added along the entire length of the outboard wings. When the flaps are deflected to 90o, the downwash on the wing is reduced to 8%. In horizontal flight the flaps are used as ailerons, this combination is known as flaperons. [3] In horizontal flight the flaperons are limited to a deflection of 35° downwards and 10° upwards. Figure 3.11.1 shows the lift curve of a NACA 65(216)-415 airfoil with and without flaperons.

A U-tail was selected for the concept, as it provides aerodynamic, stability, and structural advantages. This configuration raises the horizontal stabilizer out of the wake of the main wing, exposing it to clean airflow, which provides superior pitch control at low airspeeds. In addition, the longer moment arm provided by utilizing the full length of the vertical stabilizer allows the elevator to be lighter and less powerful. Additionally, the aircraft's rigidity is increased by the horizontal stabilizer connecting the fuselages.

The principle disadvantage of the U-tail is the possibility of a deep stall, which occurs when separated flow from the wing blankets the horizontal stabilizer. This can make the aircraft uncontrollable in a stall. However, the possibility of a deep stall is not a major concern for tiltrotor aircraft. If a deep stall is encountered, the aircraft can simply rotate the engines vertically and hover. Thus, the major disadvantage of a U-tail is mitigated for this aircraft.

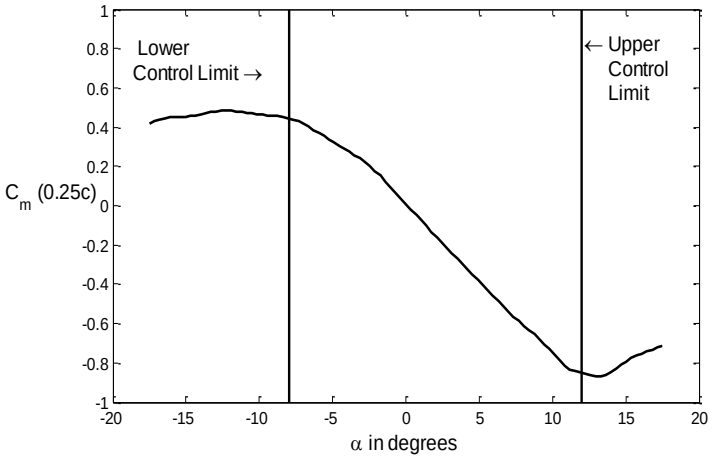

Figure 3.11.2 Moment coefficient values as a function of angle of attack

The vertical tail was designed to allow for 3°/sec per in of stick maximum roll and yaw moments. A NACA 0012 airfoil section was chosen for the vertical tail because of its symmetry and ideal thickness to chord ratio. The rudder is 25% of the chord, the resulting area of the vertical tail is 124.8 ft^2, and the maximum force applied to each tail is 6000 lbs.

The horizontal tail was designed so that the aircraft would be stable in pitch while cruising, as well as to achieve a maximum pitching moment of 4°/sec per in of stick. Using these requirements the NACA 65(216)-415 airfoil was chosen due to its favorable stall characteristics. The horizontal tail is 20 ft long and has a chord length of 7.9 ft. It is at an incidence angle of -1.2°. The elevator on the tail is 35% of the chord and can deflect 35° downward and 10° upward. The maximum force applied to the tail is 4000 lb.

The proposed V.T. R.A.F.T. project has been designed to be dynamically stable. In cruise, the aerodynamic center is located 30.2% MAC, and the neutral point is located 75% MAC, with the CG located at 68% MAC, thus the static margin is 7% MAC. Figure 3.11.2 shows the moment coefficient as a function of angle of attack. Between -12.5° and 13.5° the moment coefficient slope is negative, demonstrating that the aircraft is stable.

3.11.1 Control System

A robust control system will be needed to safely control the aircraft. The control system will be a triple redundant system that is connected to hydraulic and electrical actuators. To maintain stability, control laws will be implemented in order to limit the angle of attack of the aircraft between 11.5° and -10.5°. These limits are to ensure that the control surfaces do not loose effectiveness. Other limits to be applied to the control system will be limiting the rotation of the nacelles in horizontal flight, and prohibiting the opening of the landing gear doors when in water. In vertical flight the tilt of the nacelles as well as the rotor cyclic will be used to control the aircraft. The maximum rotation allowed structurally is 100°, and the minimum is 0°. When in horizontal flight the nacelles will be locked in place and all control of the aircraft will stem from the use of the flaperons, rudder, and elevator.

3.11.2 Transition

The most difficult flight stage for a tiltrotor aircraft is the transition between vertical and horizontal flight. The V.T. R.A.F.T. is designed to perform this task quickly and safely. The nacelles can rotate at a maximum rate of 0.667°/sec; this allows the aircraft to rotate its nacelles the full 90° in as little as 2 min and 15 sec. The aircraft must be traveling at 40 kts before nacelle rotation can safely be initiated. Once transition has begun the aircraft can transition in the minimum required time but will lose 60 ft of altitude, or it can transition in 4 min 10 sec and maintain altitude. Additionally the aircraft can transition at an even slower rate and gain altitude. For conversion, the aircraft needs to be flying at a maximum speed of 80 kts before it begins rotation of its nacelles. The conversion process takes longer since the aircraft has to slow down before it can vertically land.

3.11.3 Water Stability

Water stability was a driving constraint for the design of this aircraft and was determined through static wave analysis. The analysis assumed a worst case scenario where the wave length is the distance between the fuselages, effectively placing one fuselage would be on top of a wave and the other fuselage in the trough. The constraints for stability were keeping the rotor blades and rerouted exhaust nozzle above the water line. The maximum wave amplitude was found to be approximately 8.5 ft for both constraints. This corresponds to a sea stat of 4 (5 to 8 ft waves, and wind speeds from 17 to 27 kts), however in the case where the engines are off the aircraft can survive a sea state of 5 before receiving water damage.

3.12 Structures

3.12.1 Loading Conditions

3.12.1.1 V-n Diagram

To be able to understand the maneuvering limit loads and gust loads for the aircraft, a V-n diagram was created. Figure 3.12.1 shows the limit load factors, which were chosen to be 3 and -1, the gust load factors, and the cruise point.

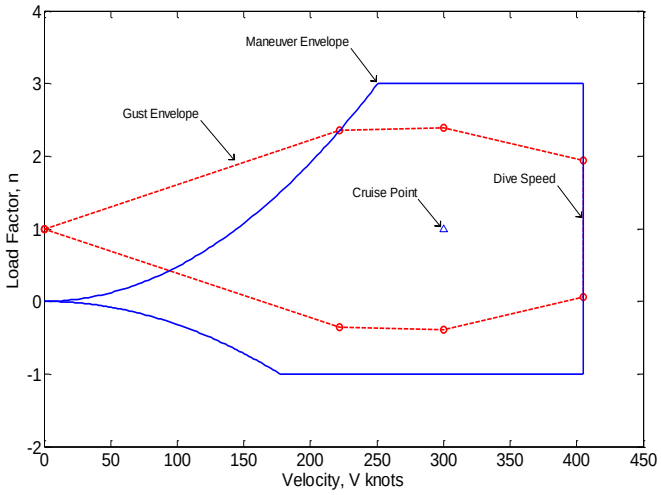

Figure 3.12.1 V-n diagram

3.12.1.2 Wing

The design of the wing box began with defining the loading conditions for the wing. The two different loading conditions that were analyzed were vertical takeoff and a 3g aerodynamic maneuver. Figure 3.12.2 depicts the wing with the takeoff thrust (W_t/2 x 1.1), engine weight (W_e), and fuselage weights (W_f) as point forces, and the wing weight (W_w/L) as an equally distributed force. Figure 3.12.3 shows the aerodynamic loading conditions, which includes the same forces as the vertical takeoff case except

that the takeoff thrust is replaced with an elliptic lift distribution. The equation for this lift distribution is depicted in Figure 3.12.3 where W_t is the GTOW and L is the length of the wing.

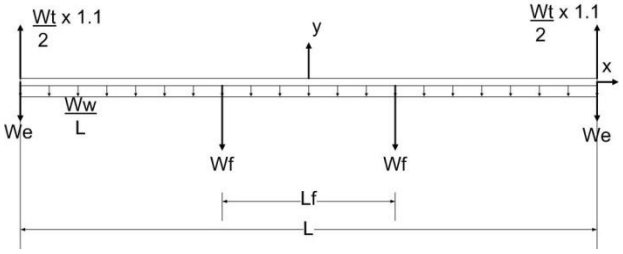

Figure 3.12.2 Loading condition for vertical take off

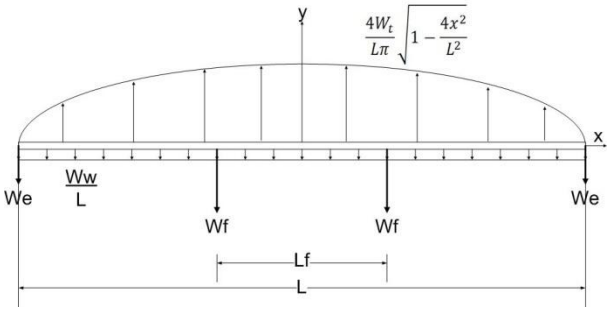

Figure 3.12.3 Loading condition for forward flight

A significant structural design constraint for any tiltrotor project is the stability boundary imposed by the proprotor, or whirl, flutter. As defined in Popelka, et alia, whirl flutter is "the instability caused by destabilizing rotor forces that are generated by the rotor flapping response to the bending and pitching motions of the low-frequency wing modes". The method described by Popelka to mitigate this problem was to use composite tailoring of the wing structure. While their method is beyond the scope of this project, the main consideration of the wing with regard to whirl flutter is the stiffness. In an attempt to do a low level mitigation of this phenomena, stiffness constraints were applied to the design of the wing structure.

3.12.1.3 Fuselage

In designing the structural components of the fuselage, the fuselage is assumed to be a beam with the weights of the components distributed along the length. Figure 3.12.4 shows these weights and their distribution along the fuselage. For aerodynamic maneuvers the fuselage is assumed to be pinned at the center of lift, which is located at 24.3 ft aft of the nose. When the fuselage is loaded with passengers, the water load shown in Figure 3.12.4 will be zero.

In addition to the aerodynamic loading case a water landing case was analyzed. In water landing the fuselage is supported by a distributed buoyancy force that results in a zero moment around the center of gravity shown in Figure 3.12.5.

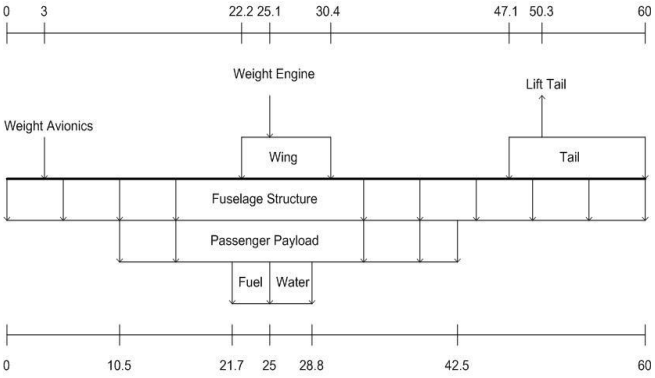

Figure 3.12.4 Fuselage load distribution in forward

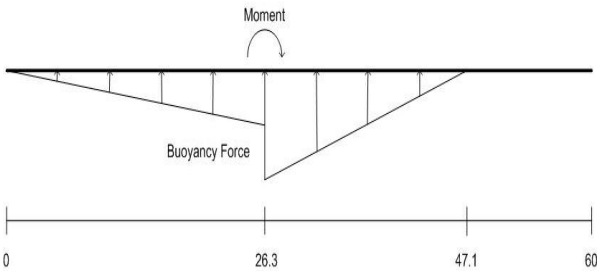

Figure 3.12.5 Water distribution loads on the fuselage

3.12.2 Wing Design

The wing was designed to satisfy the loading conditions described above, as well as stiffness requirements imposed to limit the onset of whirl flutter, the shear and moment diagrams for the critical loading conditions can be seen in Figures 3.12.6 and 3.12.7. MATLAB routines were written in order to achieve the best suitable design for the wing structure by varying all the design considerations and selecting the configuration that yielded the lightest empty weight structure. Discussed below is the design of the wing-box, which includes the spars, skin, spar caps and stringers.

The rear spar was placed at 54.3% chord, chosen to be the furthest back as to allow for the cross shaft placement and for 35% chord deflection of the flaperons. The front spar was placed to allow the maximum enclosed area between the spars to provide the largest possible torisonal stiffness. The final location of the front spar is at 16.6% chord. An idealized representation of the wing-box was formed by dimensioning the width between the spars (37.3% chord) and the height of the smaller of the two spar heights (10.7% chord).

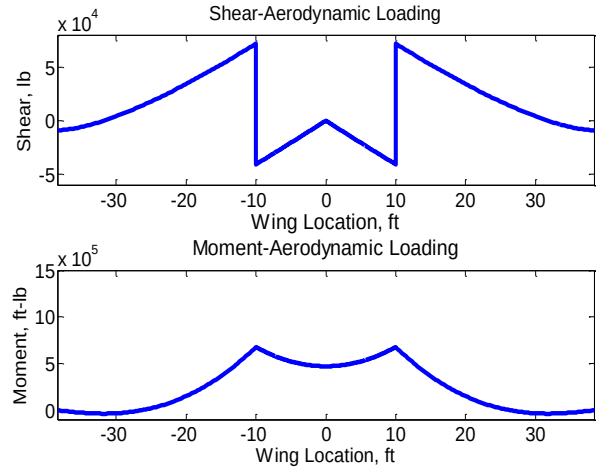

Figure 3.3.12.6 Shear and Bending Moment values along the wing span in forward flight.

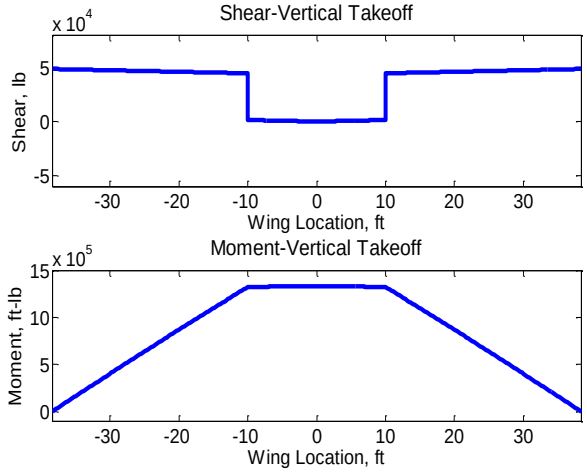

Figure 3.12.7 Shear and Bending Moment values along the wing span in vertical takeoff.

The maximum deflection of the wing during vertical takeoff was required to not exceed 6 inches to mediate whirl flutter in the design. A contour plot of the tip deflection with respect to both the root moment of inertia and the tip moment of inertia, as seen in Figure 3.12.8, depicts how wing tip deflection varies with the tapering of wing skin thickness. The blue dashed line corresponds to a linear interpolation between the untapered and infinitely tapered wing section at 6 inches of deflection. The design was required to fall above this line, with the final design point marked by the triangle.

In order to achieve the stiffness constraints imposed, it was necessary to choose a material with both a high Young's Modulus as well as high tensile and compressive yield strengths. As such, a high modulus Carbon Fiber was chosen as the primary structural material for the wing, with the exception of the spars which were to be made with an intermediate modulus Carbon Fiber as the stiffness of the spar has only minor affects to the overall wing stiffness.

A MATLAB routine varied the thickness of the skin, spars and the spacing between the ribs as well as the number of stringers and the area of these stringers with the area of the spar caps being equal to that of the stringers. The contribution made by the stringers to the total second area moment of inertia was neglected as it was considered small relative to the total inertia of the wing-box. Results of the routine are tabulated in Table 3.12.1. For the stringers a Z cross section was chosen because it allows easy maintenance and high moment of inertia to area ratio.

Table 3.12.1 Final results for wing box design

Num of Stringers	6
Rib Spacing	2.0 ft
Area of Stringers	.01 ft^2
Spar Thickness	.0075 ft
Root Skin Thickness	.0233 ft
Tip Skin Thickness	.005 ft

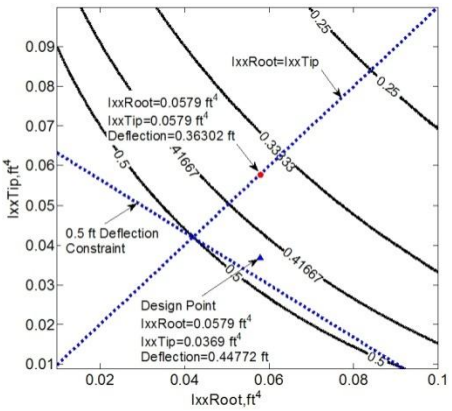

Figure 3.12.8 Contour Plot of Wing Deflection

A structural CAD model of the outboard wing was constructed to validate the results and analyzed using ANSYS Static Structural for the vertical takeoff loading condition. The model used did not include the tapering of the wing skin and so it is expected that the deflection of the wing would be significantly less than 6 inches. Figure 3.12.9 shows the results from the simulation and that the maximum deflection is 4.73 inches. The wing deflection result was compared with the contour plot for an untapered wing, seen in Figure 13.12.8 and marked by the call out, and shows that the two models agree. ANSYS also showed no region of structural failure for this loading condition.

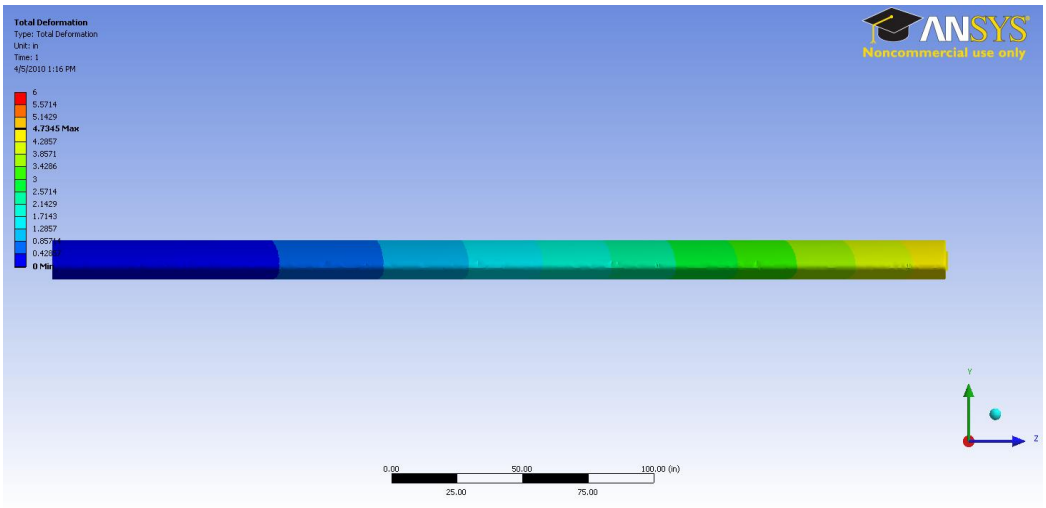

Figure 3.12.9 ANSYS results for tip deflection along outer wing section

3.12.3 Strut Feasibility Study

A strut feasibility study was performed in the initial stages of the wing box design to determine if a strut would be beneficial. The method of designing the wing box with the strut was similar to the normal wing except that the wing was broken up into an outboard wing and inboard wing section. Two wing sections were used because it was discovered that the strut imparted a very large moment on the center wing causing the stresses to be much larger than on the outboard wing. Table 3.12.2 shows the results of the initial wing box design, without tapering and material change and the strut braced wing box design. The total strut braced wing weight, including the weight of the struts, was found to be 5579 pounds. The strut was found to not be beneficial because it was only going to decrease the weight of the aircraft by 160 pounds while adding complexity and detrimental effects to the aerodynamics of the aircraft.

Table 3.12.2 Results of the strut feasibility study

	Semi-monocoque	Strut Braced Wing (Outboard)	Strut Braced Wing (Inboard)	Strut
Thickness Flange	0.0475 ft	0.019 ft	0.095 ft	N/A
Thickness Web	0.0390 ft	0.018 ft	0.021 ft	N/A
Area Wing Box	0.4191 ft^2	0.1812 ft^2	0.7951 ft^2	0.1 ft^2
Wing Spar Weight	5739 lb	1836 lb	2835 lb	454 lb
# of Stringers	4	4	9	N/A
Rib Spacing	2 ft	2 ft	1.83 ft	N/A
Area Stringer	0.0035 ft^2	0.001 ft^2	0.0025 ft^2	N/A

3.12.4 Fuselage Structure Design

3.12.4.1 Methods

The methods that were used to design the fuselage members of the aircraft are outlined in Design of Aircraft by Thomas C. Corke. The first step was to determine the loads on the fuselage as shown in Figure 3.12.4. The tail lift for straight and steady level flight was then determined from the loads acting on the fuselage., Shear and bending moment calculations were completed once all the loads were known and the max bending moment was found. The minimum skin thickness for the fuselage was then found according to equation 3.12.1,

$$t_{min} = \frac{4*M*n_{design}}{\pi*\sigma_{Tu}*(A*B+A^2)} \quad (3.12.1)\ ^{(14)}$$

where M is the maximum bending moment, n is the design load factor, σ_{Tu} is the ultimate tensile strength of the material chosen, and A and B are the major and minor axis radii of the fuselage cross section. The minimum skin thickness of different materials was then compared.

The bulkhead spacing and the longeron cross sections were designed using equation 3.12.2,

$$\frac{L^2}{I_l*R} < \frac{C*\pi^2*E}{0.154*n_{design}*M} \quad (3.12.2)\ ^{(14)}$$

where L is the distance between bulkheads, I_l is the moment of inertia of the longerons, R is radius of the cross section of the fuselage, C is a factor that depends on how the column is fixed at its ends and was set equal to 1, E is the modulus of elasticity of the longeron material, n_{design} is the design load factor, and M is the maximum bending moment.

A different load factor was used in equations 1 and 2 to analyze water landing. The equation that was used to calculate the water landing load factor is detailed in FAR Part 25.527.

3.12.4.2 Results

The shear and bending moment diagrams for the two loading cases described in the fuselage loading conditions section can be seen in Figures 3.12.10 and 3.12.11. These figures show that during a water landing the fuselage experiences much lower shear and moment forces. The water load factor that was calculated in accordance with FAR Part 25.527 was found to be 8.34; which is almost double the design load factor of 4.5. The water landing case resulted in smaller values for the fuselage members; therefore the aerodynamic loading case was used as the limiting case for design.

Multiple materials were considered when calculating the minimum skin thickness for the fuselage. The minimum skin thicknesses that were found ranged from 0.0042 inches for the Carbon Fiber to 0.0323 inches for 6061-T6 Aluminum. The skin thickness values calculated was less than the 0.05 inch thickness required to permit countersinking for flush rivets. The minimum skin thickness is therefore 0.05 inches. 6061-T6 Aluminum was chosen as the skin material because it is cheaper than carbon fiber, the higher strength of the Carbon Fiber is not needed, and it has the lowest density of the Aluminum materials tested.

The design of the longerons and the spacing of the bulkheads are dependent upon each other so therefore it was chosen to fix the bulkhead spacing and design the longerons to support that spacing. The bulkhead spacing was chosen to be 5 ft so that the side loading door would not interfere with any of the bulkheads. The cross section of the longerons was chosen to be a "T" shape with the width equal to the height and the same thickness throughout for simplicity and maintenance reasons. The number of longerons in a 90 degree arc around the fuselage longitudinal axis was chosen to be 4 based upon the methods discussed in *Design of Aircraft*. Finally the width and thickness of the longerons were designed for the same materials used for the fuselage skin. The Carbon Fiber resulted in the minimum cross sectional area, but because of the higher cost, 2024-T3 Aluminum was chosen because it had the lowest cross sectional area of the Aluminums. The final values for the width and thickness of the longerons were calculated to be 3 inches and 0.0629 inches.

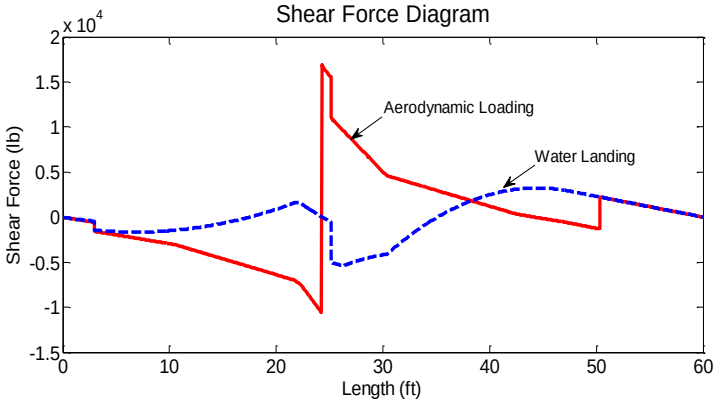

Figure 3.12.10 Fuselage shear force diagram

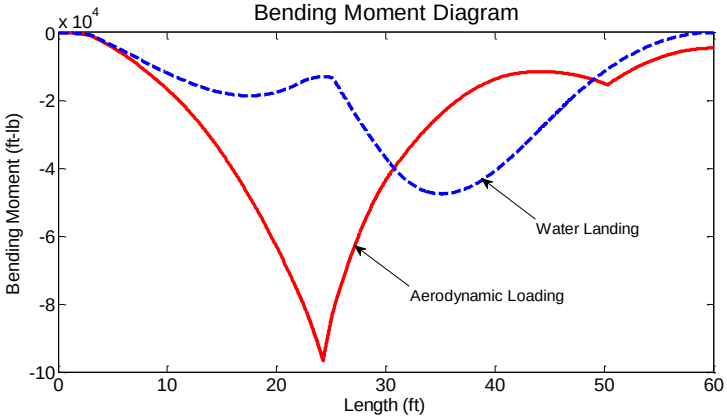

Figure 3.12.11 Fuselage bending moment diagram

3.13 Systems

3.13.1 Fuselage Layout

3.13.1.1 Cabin Seating

V.T. R.A.F.T. will use the same new troop seats added to the V-22 by Golan Industries/Army Division. This will allow for 25 passengers and 2 flight crew in each fuselage as

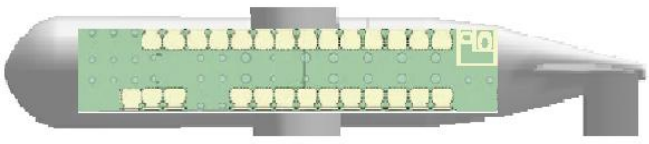

Figure 3.13.1 Right fuselage cabin layout

seen below in Figure 3.13.1**.** The right fuselage will also have the addition of two crew seats for the pilots and the left fuselage will have an additional seat in the nose for the primary flight medic. The crew chief's seat is installed just aft of the cabin on the left side. A restroom located at the rear of the of each cabin.

3.13.1.2 Cockpit Interface

The cockpit of the V.T. R.A.F.T. is the most complex station within the aircraft. The physical aspects (seats and furnishings), mechanical flight controls (throttle controls, control pedals, control stick, etc.), instrument controls (avionics and aircraft systems) and the informational interfaces (various digital displays) make up the cockpit interface as shown in Figure 13.13.2. The cockpit interface utilizes electronic cockpit displays instead of traditional instruments to allow for customization of system indicators on each multifunction display. The use of an electronic interface allows maximum flexibility to incorporate new technologies into the aircraft, thus increasing the longevity of the system. The cockpit features a heads up display (HUD) for the pilot and copilot to allow for quick access for vital flight data.

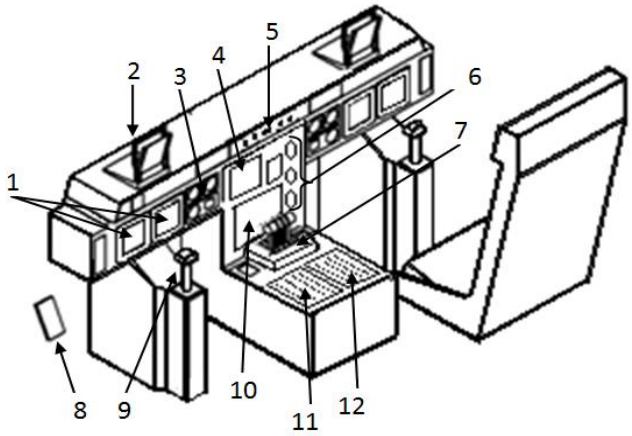

1	Multifunctional Displays
2	HUD
3	Misc. Switches
4	Standby Flight Display
5	Flight director
6	Altimeter and Airspeed
7	Throttle Controls
8	Control Pedals
9	Control Stick
10	Engine Instrument Alert Sys.
11	ECS and Landing Gear Controls
12	Lights, Icing and Radio Controls

Figure 3.13.2 Cockpit Layout

3.13.1.3 Cargo Capabilities

The cargo floor is made of multiple panels of composite honeycomb material that is 4in thick. The cargo floor is installed with tie- down rings that lie flush with the surface when not in use. Cargo is loaded via a sliding 5 x 5 ft exterior door. The internal cargo handling system is modeled after the V-22 and is comprised of a roller style conveyor system with guide rails and a cargo winch with a 2,000 lb capacity and speed of 30 fpm. Compartments for tiedown straps and barrier netting are located at the rear of the fuselage next to the restroom. Since cargo is loaded through the exterior sliding door cargo, cargo is limited to the 40 x 48 in pallets. However, it can accommodate some of the US Marine Corps family of internally transportable vehicles designed for the V-22 or any cargo that is no larger than 70 x 60 x 60 in.

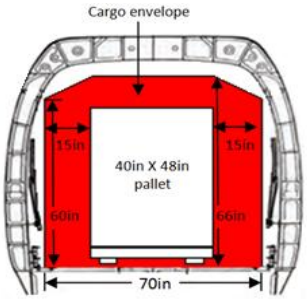

3.13.3 Cargo Envelope

3.13.2 Flight Control System (FCS)

The FCS, shown in Figure 3.13.4 for the V.T. R.A.F.T. is a fly-by-wire system. The digital control offers a smooth transition between rotary wing and fixed wing flight. There is a triple- redundant Flight Control Computer (FCC) located in the fuselage. The FCC automatically determines inputs to control systems based on the current aircraft orientation. Specific power requirements for needed engine performance are sent via digital bus to the two Full Authority Digital Engine Controllers (FADEC) within each engine. An Automatic Flight Control System (AFCS) integrated with the avionics allows for a closed loop control guidance or autopilot.

3.13.3 Electrical System

Multiple AC and DC systems, AC/DC convertors, lead for redundancy, a single lead acid battery, frequency generators, and interior/exterior lighting make up the electrical system of the aircraft. A single lead acid battery, which provides 24 VDC, is installed to provide utility DC power to start the Hamilton Sundstrand Power System T-62T-46-2 APU and provide in-flight emergency power in the case the APU needs restarting. DC buses remain at 28VDC at all times in order to reduce wire weight by permitting increased voltage loss. [10] Four Honeywell 90 kVA generators are connected to a converter to provide the primary electrical power necessary for aircraft systems function properly flight.

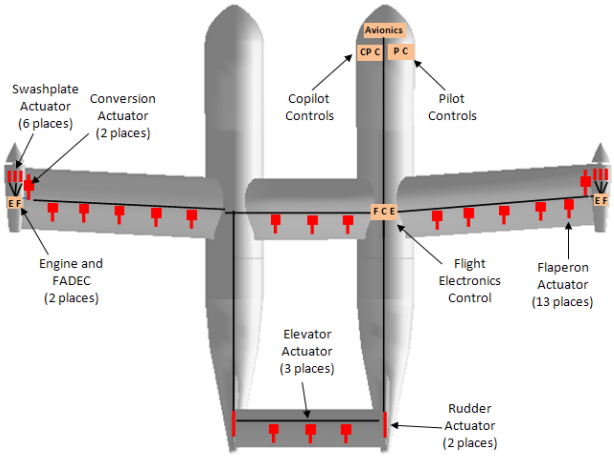

Figure 3.13.4 Flight Control System Mapping

3.13.4 Hydraulic System

The hydraulic system of the V.T. R.A.F.T. is composed of two primary systems and backup utility system. The return components of the hydraulic systems are packaged in modules which reduces the number of hydraulic lines, individual components, and leak points. All of this leads to decrease in possible system failure. [10]

3.13.5 Environmental Control System (ECS)

A modern ECS is installed within the aircraft to ensure passenger and crew health is maintained over the entire mission profile. Oxygen-enriched air for crew breathing is provided at six stations in each fuselage to allow the aircraft to operate without passengers at altitudes above 10,000 ft. In the event of oxygen failure to either fuselage there are two emergency oxygen kits that are capable of supporting four people each.

Anti-icing is provided for the main cabin windshield, engine inlets, rotor blades and pitot probes. A heating system designed by GKN Aerospace will be incorporated on the V.T. R.A.F.T. to control icing on the wings. [15] The system is made of multiple layers of composite heating mats. These mats are more efficient than traditional deicing systems and extend airframe performance. Electronic heating elements are used to deice the rotor blades and engine components. Sensors are used to automatically initialize deicing during flight.

3.13.6 Fuel System

The fuel system is integrated into the wing and the subfloor resulting in 18 tanks as seen in Figure 3.13.5. The wing fuel tanks occupy 35% of the chord, as seen in Figure 3.12.6, and are made of a lightweight synthetic rubber able to withstand a significant drop. Subfloor tanks are crash resistant, partially self-sealing and made of light weight aluminum. As fuel is used the nitrogen-rich air is provided to the tanks, reducing the possibility of a fuel air explosion. Two boost pumps are located in the subfloor and one in each wing to ensure fuel is evenly moved to the feed tanks. The fuel system is linked directly to the FCS to allow for the ability to relocate fuel in order to aid in balancing the aircraft. As fuel is used, the fuel located the closet to the center of the aircraft is pumped outboard to the engines. The V.T. R.A.F.T. uses a gravity drain for defueling in emergency situations.

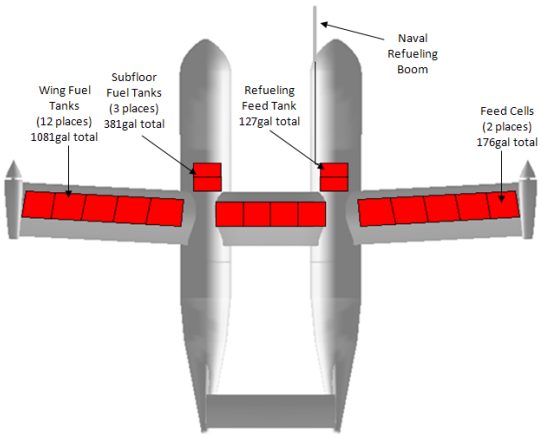

Figure 3.13.5 Fuel Tank Layout

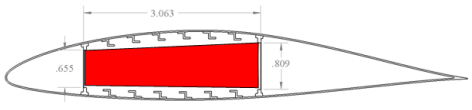

Figure 3.13.6 Fuel tank location in wing box

A retractable drogue aerial refueling system is outfitted on the aircraft to increase mission radius. The refueling probe is attached to the left side of the right fuselage, extends 110 inches in front of the nose while deployed, and six inches when retracted. The probe can

be controlled electronically or manually. In addition to aerial refueling, this aircraft is capable of being refueled on the ground via pressurized and gravity refueling.

3.13.7 Firefighting System

Two storage tanks are capable of carrying 1500 gal (750 gal in each fuselage) of water. Two American Turbine AT-309 pumps allow the tanks to be filled while in the water or hovering up to ten feet above the water via a six inch diameter hose. The pumps can be individually controlled when the aircraft is on the water to provide precise surface maneuvering, even with the main engines off. This is highly desirable during surface rescue operations. The surface performance is achieved through controlling two flutter valves located forward and aft of each pump. The first valve controls whether water is directed into the aircraft via hose or directly from the undercarriage. The second valve directs the water directly out of the aircraft or into the storage tanks. Water is released through a 20 x 35in door located just forward of the main landing gear.

The American Turbine AT-309 pumps also provide an extra source of maneuverability in the water. Through the use of flutter valves, located immediately forward and aft of the pump, the pumps can function as impellers. This allows V.T.R.A.F.T to precisely taxi in the water with the engines off, as well as providing the ability to turn the aircraft in a small space by having one pump run forwards and one in reverse. This is designed to enhance the safety and convenience of surface rescue operations.

3.13.8 Rescue and Emergency Capabilities

3.13.8.1 Rescue Winches and Placement

Rescue winches will be outfitted on the aircraft to enable rescue operations in hover. The current provider for all rescue winches in military aircraft is Goodrich. The Goodrich 42305 is an internal model which provides 600 lb of lift and 200 ft of useable cable length. [16] Two winches will be located in each fuselage centered above each door. The winches located at the center of the aircraft will be used primarily because the cables are shielded from the downdraft of the engines.

3.13.8.2 Aeromedical Operations

A full medical bay is located in the nose of the left cockpit. The medical bay will be equipped similarly to a medical evacuation helicopter. Each fuselage will be equipped with basic medical equipment as well. Additionally, the weight from the medical bay provides a counter balance to the avionics located in the right fuselage. The aircraft can also be equipped with 36 litters. Litters are arranged lengthwise in 12 banks of three high.

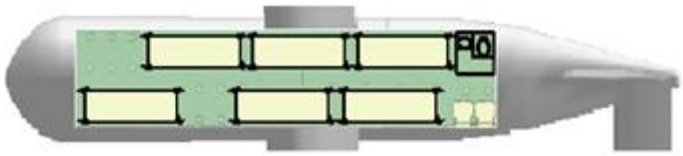

Figure 3.13.7 Top view of litter configuration

3.13.9 Landing Gear

The landing gear for each fuselage is a bicycle configuration along the center line of each fuselage. The nose landing gear is a single wheel gooseneck design, whereas the main landing gear consists of two wheels. The main gear is positioned 35º from the vertical aft of the center of gravity, which is comparable to the V-22. [10] The angle is a compromise between aircraft and helicopter configurations. With this configuration, the nose landing gear carries 33.7% of the static TOGW and the main gear carries 66.3%. The aircraft has a wheel track of 22.5 ft, producing a turn-over angle of 26º and a tail-strike angle of 15º. The bicycle landing gear configuration reduces the number of landing gear sets needed, thus reducing weight. Both the nose and main gear retract aft into the fuselage due to spacing constraints in the subfloor.

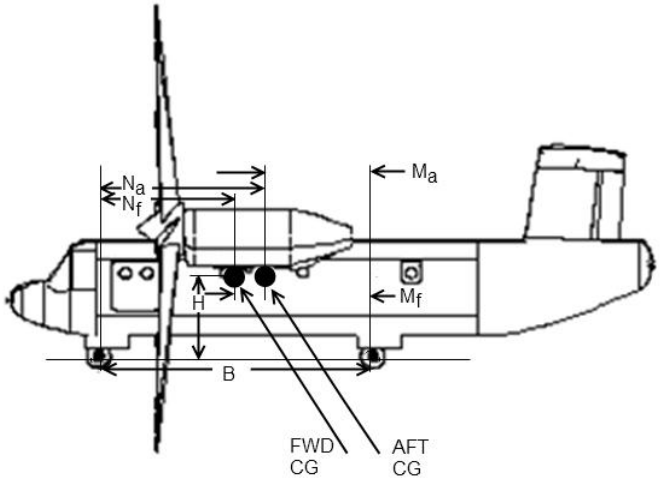

Figure 3.13.8 Landing gear geometry schematic [7]

Table 3.13.1 shows the numerical analysis results for calculating the loads on each wheel**.** Figure 3.13.8 shows the geometry that depicts the load coefficients. Based on Figure 3.13.8 the V.T. R.A.F.T. more than meets standards set forth by FAR 25 thus allowing for later growth of the aircraft.

Table 3.13.1 Landing gear data used to determine the design loads for the landing gear

Location Forward CG (ft)	25.05	Ma (ft)	1.57
Location Aft CG (ft)	27.55	Mf (ft)	4.07
Location nose LG (ft)	5	Max Static Load (main, lb)	65443
Location main LG (ft)	29.12	Max Static Load (nose, lb)	11811
Number of nose wheels	2	Min Static Load (main, lb)	58188
Number of rear wheels	4	Min Static Load (nose, lb)	4556
TOGW (lb)	**70000**	Dynamic Braking Load (nose, lb)	5858
Na (ft)	22.55	Load per nose tire (lb)	5905
Nf (ft)	20.05	Load per main tire (lb)	16360
B (ft)	24.12	7% margin nose tire (FAR 25, lb)	6319
H (ft)	6.5	7% margin rear tire (FAR 25, lb)	17506

Table 3.13.2 Data sheet on selected tires [17]

	Size	Speed (mph)	Max Load (lb)	Max Pressure (psi)	Max width (in)	Max diam. (in)	Wheel diam. (in)	PLY Rating
Front tire	21 x 7.25-10	210	6400	166	7.2	21.25	10.0	12
Main tire	27.75 x 8.75-14.5	225	21500	320	8.75	27.75	14.5	24

3.14 Cost

To get an approximate cost analysis for V.T. R.A.F.T., the method described in Chapter 18 of Raymer was used. This method is based primarily on the empty weight, maximum speed, the desired production output in five years, number of flight test aircraft, cruise velocity and take off gross weight. Using these values along with the current wrap rates for engineering, tooling, quality control, and manufacturing an estimate for the Research, Development, Test and Evaluation (RDT&E) plus flyaway cost was determined. In addition to this cost the operation and maintenance costs were estimated. The operation and maintenance costs were estimated by the fuel cost, crew cost and total maintenance cost. Based on this analysis the RDT&E plus flyaway cost was found to be $52,603,000 per aircraft, and the operation and maintenance cost was $3,216,000 per year. The detailed cost estimation table can be seen in Appendix B.

4. Conclusion and Recommendation for Further Study

One area of concern was the effect of splashing while hovering directly above water. It was feared that the downwash from the rotors might cause the engines to ingest water spray. In order to study this effect a full size rotor and engine assembly could be operated at maximum power directly over water and the thrust from the rotors monitored to ensure no water is ingested in the engine. Other areas of concern are wing flutter and autorotation. The wings should be tested at all flight conditions to ensure that flutter does not occur. Autorotation is the ability of the rotors to produce lift and therefore slow descent even in an engine out situation. It is often represented in a height velocity diagram also known as a "Dead Man's Curve". Due to the large rotors, the autorotation performance of the VT R.A.F.T is anticipated to be superior to the V-22. This should be verified in simulator tests at a variety of altitudes and airspeeds, as well as during flight testing.

References

1. **Qantas Airways Limited ABN.** The Catalinas. [Online] [Cited: 09 06, 2009.] http://www.qantas.com.au/travel/airlines/history-catalinas/global/en.
2. **Houbolt, John C.** *Why Twin-Fuselage Aircraft?* 1982. pp. 26-35.
3. **Bell Boeing V-22 Program Office.** *V-22 Osprey Pocket Guide.* Amarillo : Bell Boeing, 2007.
4. **Romander, Nathan.** *3-D Navier- Stokes Analysis of Blade Root Aerodynamics for a Tiltrotor Aircraft in Cruise.* Moffet Field, CA : Nasa Ames Research Center, 2006.
5. **Global Security.** Seaplanes. [Online] [Cited: 9 9, 2009.] http://www.globalsecurity.org/seaplanes.
6. —. X-19 [C-143]. [Online] [Cited: 9 7, 2009.] http://www.globalsecurity.org/military/systems/aircraft/x-19.htm.
7. **Raymer, Daniel.** *Aircraft Design: A Conceptual Approach.* Reston : AIAA, 2006.
8. **Rolls- Royce.** AE 1107C- Libery turboshaft. [Online] March 2009. www.rolls-royce.com.
9. **Leishman, J. Gordon.** *Priciple of Helicopter Aerodynamics.* Cambridge : Cambridge Press, 2000.
10. **Bell Boeing.** *V-22 Product Information (Rev. B).* 2009.
11. **Roskam, Dr. Jan.** *Airplane Design Part V: Component Weight Estimation.* Lawrence : Design, Analysis and Research Corporation, 2003.
12. **Gur, Ohad, Mason, William H and Schetz, Joseph A.** *Full Configuration Drag Estimation.* San Antonio : AIAA Paper 2009-4109, 2009.
13. **Marchman, J.M.** *Introduction to Aerodynamics & Aircraft Performance.* s.l. : Virginia Tech, 2004.
14. **Corke, Thomas.** *Design of Aircraft.* Upper Saddle River : Prentice Hall, 2003.
15. **Donaldson Company.** Filtration Systems. *Donaldson Company.* [Online] [Cited: April 11, 2010.] http://www.donaldson.com/en/index.html.
16. **Goorich Hoist and Winch.** [Online] http://www.hoistandwinch.com/customersupport.
17. Aircraft Tire Data Book. [Online] October 2002. [Cited: April 11, 2010.] http://www.goodyearaviation.com/resources/pdf/datatires.pdf.
18. **Global Security.** V-22. [Online] [Cited: 9 7, 2009.] http://www.globalsecurity.org/military/systems/aircraft/v-22.htm.
19. **Ogata, Katsuhiko.** *System Dynamics.* Upper Saddle River : Prentice Hall, 2004.
20. **Popelka, David, et al.** *Results of an Aeroelastic Tailoring Study for a Composite Tiltrotor Wing.* Fort Worth : American Helicopter Society, 1995.
21. **Maiisel, Martin, Giulianetti, Demo and Dugan, Daniel.** *The History of the XV-15 Tilt Rotor Research Aircraft.* Washington D.C. : NASA, 2000. SP-2000-4517.

Appendices

Appendix A: Weight Estimation

Table 3.13.2 Weight Estimation Table [17]

Component	Weight	Longitudinal Location	Moment
	(lb)	(ft)	(ft-lb)
Passengers(200 lb each)	10,000	30.3	303000
Crew(200 each)	1,200	8.2	9840
Medical Equipment	500	3.1	1550
Wing Fuel Weight	8,975	24.8	222580
Fuselage Fuel Weight	1,200	34.3	41160
Empenage	3,134	54.9	172057
Avionics	1,213	3.1	3760
Propulsion System (4480 lb each)	8,962	26.3	235701
Front Landing Gear	1,786	5.3	9466
Main Landing Gear	2,690	29.1	78279
Fuselage	15,678	24.3	380975
Seats	1,848	30.3	55994
Wing Weight	5,275	24.8	130820
Total	62,461		1645182
X-Direction Center of Gravity	26.3	ft	

Appendix B: Cost Estimation

Cost Analysis for V.T.R.A.F.T.						
Empty Weight (We)	38761	lbs		Fuel Price	2.94	dollars/gal
Max Speed (V)	330	knots		Fuel Burned/Hour	385.3	gallons/hour
Number of Planes in 5 years (Q)	50	planes		Flight Hours/Year	700	hours/year
Number of Flight Test Aircraft (FTA)	6	planes		**Fuel Cost/Year**	**792947.4**	**dollars/year**
Cruise Velocity (Vc)	300	knots				
TOGW (Wo)	62461	lbs		One-Man Crew Cost	183.5629588	dollars/block hour
	Wrap Rates			Crew	6	
Engineering (RE)	86	dollars		**Crew Cost/Year**	**770964.427**	**dollars/year**
Tooling (RT)	88	dollars				
Quality Control (RQ)	81	dollars		Maintenance Man Hours/Flight Hour	20	
Manufacturing (RM)	73	dollars		Maintenance Man Hours/Year	14000	hours/year
				Maintenance Labor Cost	1022000	dollars/year
Avionics Cost (Cavionics)	10000000	dollars		Aircraft Cost Less Engine (Ca)	48603409.69	dollars
Total Production Quantity times # Engines (Neng)	100			Cost Per Engine (Ce)	2000000	dollars
				Number of Engines (Ne)	2	
Enge Hours (HE)	6029797.622	hours		Material Cost/Flight Hour	364.591252	dollars/hour
Tooling Hours (HT)	3485977.099	hours		Material Cost/Year	255213.8764	dollars/year
Mfg Hours (HM)	8668658.32	hours		**Total Maintenance Costs**	**1277213.876**	**dollars/year**
QC Hours (HQ)	1152931.557	hours				
Devel Support Cost (CD)	96449702.04	dollars		**Operation And Maintenance Cost**	**2841125.703**	**dollars/year**
Flight Test Cost (CF)	57542936.88	dollars				
Mft Materials Cost (CM)	224649751.7	dollars				
Engine Production Cost (Ceng)	2000000	dollars				
RDT&E+flyaway Costs	**2630170484**	**dollars**				
RDT&E+flyaway Costs Per Aircraft	**52603409.69**	**dollars**				

Appendix C: CAD drawings

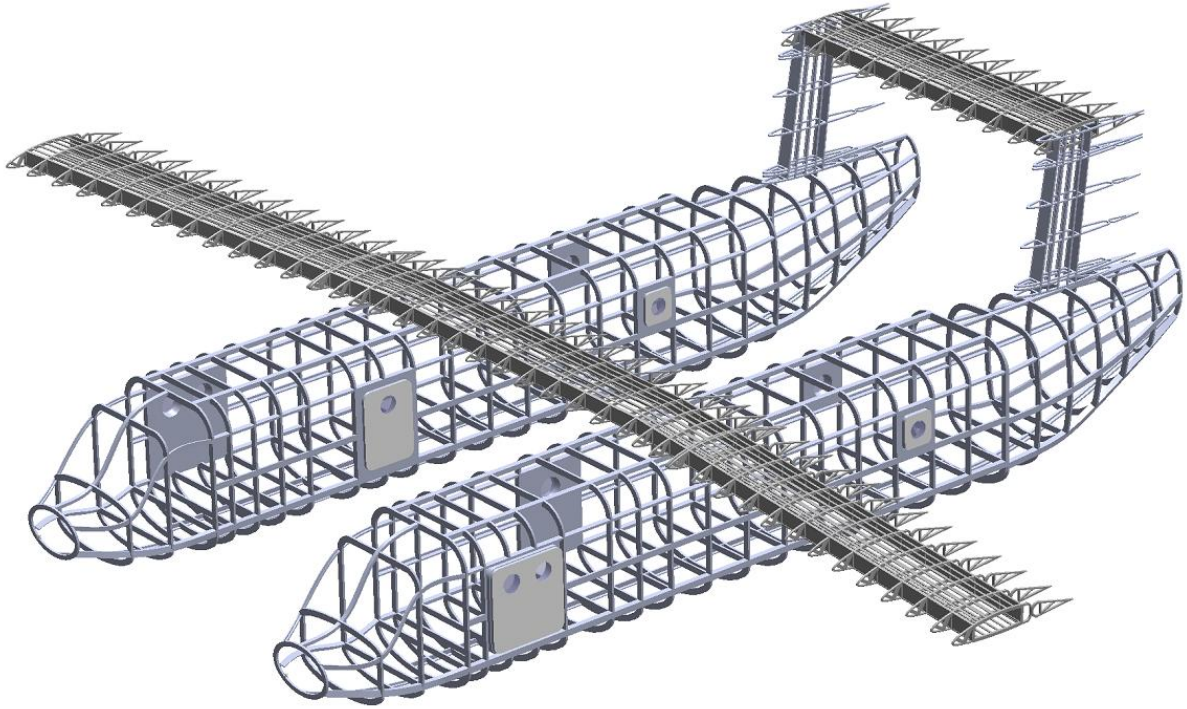

Figure C.1. Structural Design of V.T. R.A.F.T.

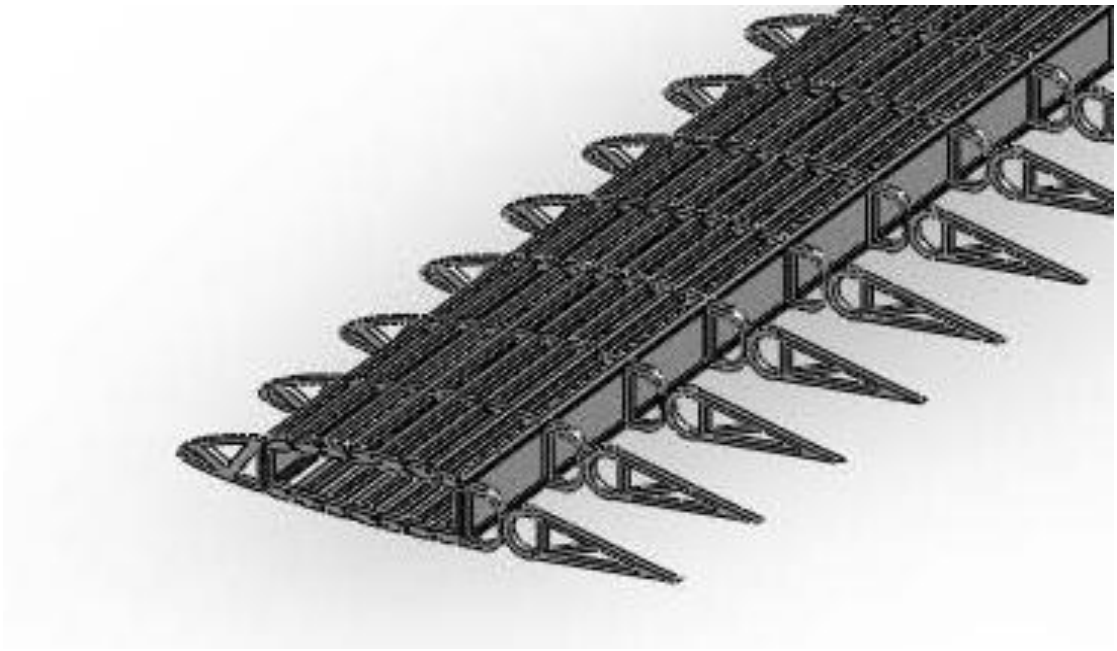

Figure C.2. Structural Design of Wing

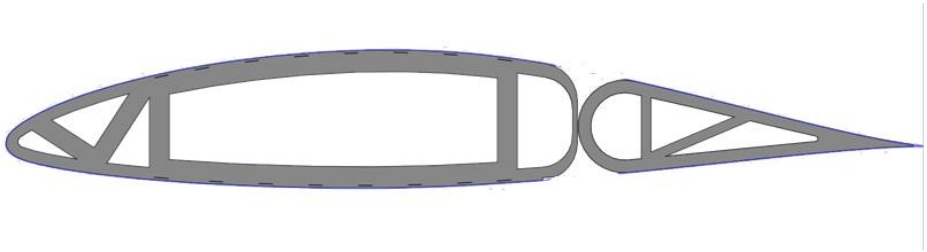

Figure C.3. Structural Design of a wing rib with flaperon

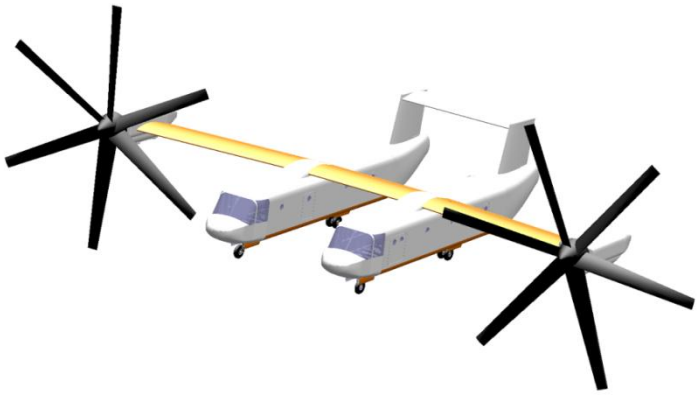

Figure C.4. V.T. R.A.F.T. in airplane mode

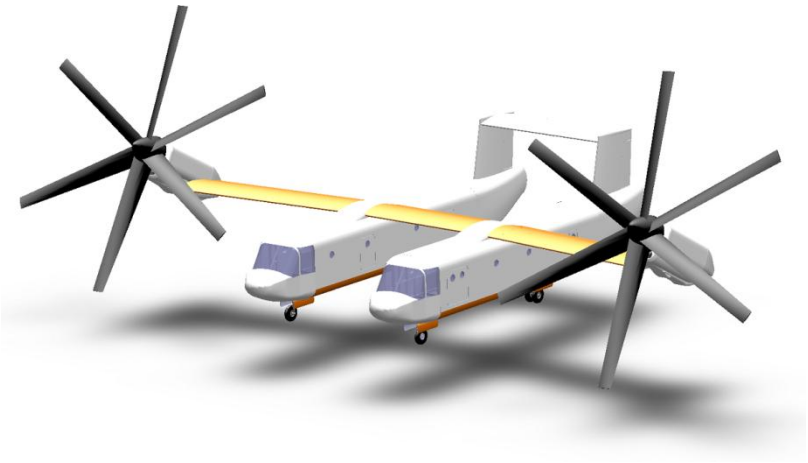

Figure C.5. V.T. R.A.F.T. with nacelles rotated 40°

Figure C.6. V.T. R.A.F.T. in helicopter mode